Identification of a novel subfamily of bacterial AAT-fold basic amino acid decarboxylases and functional characterization of its first representative: *Pseudomonas aeruginosa* LdcA

Diego Carriel-Lopez,[1,2,#] Pierre Simon Garcia,[3,4,#] Florence Castelli,[5] Patricia Lamourette,[5] François Fenaille,[5] Céline Brochier-Armanet,[3,4,*] Sylvie Elsen[2,] and Irina Gutsche[1,***]**

[1]University of Grenoble Alpes, CNRS, CEA, CNRS, IBS, F-38000 Grenoble, France

[2]Biology of Cancer and Infection, U1036 INSERM, CEA, University of Grenoble Alpes, ERL5261 CNRS, Grenoble, France

[3]Université Lyon 1, CNRS, UMR5558, Laboratoire de Biométrie et Biologie Évolutive, F-69622, Villeurbanne, France

[4]MMSB Molecular Microbiology and Structural Biochemistry, Institut de Biologie et de Chimie des Protéines 69367 LYON cedex 07, France

[5]Service de Pharmacologie et Immuno-Analyse (SPI), Laboratoire d'Etude du Métabolisme des Médicaments, CEA, INRA, Université Paris Saclay, MetaboHUB, F-91191 Gif-sur-Yvette, France

For correspondence. *E-mail celine.brochier-armanet@univ-lyon1.fr; Tel. (33) 426234476; Fax (33) 472431388; **E-mail sylvie.elsen@cea.fr; Tel. (33) 438783074; Fax (33) 438785058; ***E-mail irina.gutsche@ibs.fr; Tel. (33) 457428766; Fax (33) 438785122.

Short Title: LdcA, a new phylogenetic family of bacterial Ldcs

Key words: bacterial amino acid decarboxylases, polyamines, evolution, lysine decarboxylase, *Pseudomonas aeruginosa*

[#]These authors contributed equally to this work

Summary

Polyamines are small amino-acid derived polycations capable of binding negatively charged macromolecules. Bacterial polyamines are structurally and functionally diverse, and are mainly produced biosynthetically by PLP-dependent amino acid decarboxylases referred to as LAOdcs (Lysine-Arginine-Ornithine decarboxylases). In a phylogenetically limited group of bacteria, LAOdcs are also induced in response to acid stress. Here, we performed an exhaustive phylogenetic analysis of the AAT-fold LAOdcs which showcased the ancestral nature of their short forms in *Cyanobacteria* and *Firmicutes*, and emergence of distinct subfamilies of long LAOdcs in *Proteobacteria*. Complex evolutionary history of these subfamilies and their relationships were disclosed. Moreover, we identified a novel subfamily of lysine decarboxylases, LdcA, ancestral in *Betaproteobacteria* and *Pseudomonadaceae*. Thus, we analyzed expression of LdcA from *Pseudomonas aeruginosa*, and uncovered its role in promoting growth and reducing persistence of this multidrug resistant human pathogen during carbenicillin treatment, intimately linked to cadaverine production. Finally, we documented a certain redundancy in the function of the three main polyamines - cadaverine, putrescine and spermidine – in *P. aeruginosa* by demonstrating the link between their intracellular level, as well as the capacity of putrescine and spermidine to complement the growth phenotype of the *ldcA* mutant.

Introduction

Polyamines are small amino acid-derived molecules with two or more amino groups separated by alkyl chains (Lightfoot & Hall, 2014, Tabor & Tabor, 1964). They perform essential functions

in all living organisms by participating in DNA replication, gene expression and protein synthesis, and are generally described as growth factors (Lightfoot & Hall, 2014, Michael, 2016b). At physiological pH, polyamines behave as polycations and can interact with negatively charged macromolecules such as nucleic acids, membrane phospholipids and proteins (Tabor & Tabor, 1964, Tabor & Tabor, 1985). They were proposed to bind and structurally modify RNA thereby acting at the level of translation (Igarashi, 2006, Igarashi & Kashiwagi, 2015). Strengthening this hypothesis, "polyamine modulons" were identified in *Escherichia coli* and more recently in eukaryotes (Igarashi, 2006, Igarashi & Kashiwagi, 2015). As a possible consequence, bacterial polyamines were shown to participate in expression of proteins essential for growth fitness and viability but also in processes such as biofilm formation, antibiotic resistance and virulence (Michael, 2016a, Di Martino *et al.*, 2013, Karatan & Michael, 2013, Kwon & Lu, 2006, Shah & Swiatlo, 2008).

The triamine spermidine (Spd), essential in eukaryotes and archaea (Michael, 2016b, Lightfoot & Hall, 2014, Michael, 2016a), and its diamine precursor putrescine (Put) are extensively studied because these two polyamines are the only ones produced in all eukaryotes (Michael, 2016a, Michael, 2016b). In bacteria, the polyamine repertoire and hence their roles are the most diverse. In particular, a third widespread bacterial polyamine, cadaverine (Cad), appears increasingly important for the physiology of *Proteobacteria*. Cad is recognized as an important player in enterobacterial acid stress response wherein it decreases porin permeability to protons and alkalinizes the medium (Dela Vega & Delcour, 1996, Zhao & Houry, 2010). During oxidative stress response, Cad is also capable of scavenging reactive oxygen species (ROS) in *Vibrio vulnificus* (Kang *et al.*, 2007). In some Negativicutes, *Selenomonas ruminantium* and

Veillonella sp., Cad was shown to be incorporated in the peptidoglycan and essential for its stability (Kamio *et al.*, 1986, Kamio & Nakamura, 1987). Finally, this polyamine is involved in iron uptake and is required for the synthesis of hydroxamate-type siderophores in different bacterial species such as *Streptomyces coelicolor* (Burrell *et al.*, 2012).

Polyamine biosynthesis depends on the activity of basic amino acid decarboxylases using Lysine, Arginine or Ornithine as specific substrate to produce Cad, Agmatine (Agm) or Put, respectively. These enzymes can therefore be generally referred to as LAOdcs (Lysine-Arginine-Ornithine decarboxylases). In most eukaryotes, Put synthesis is carried out by an Odc. An alternative pathway for Put biosynthesis found in bacteria and plants involves decarboxylation of arginine by arginine decarboxylases (Adc); these enzymes produce Agm which is further converted into Put by agmatine iminohydrolase/deiminase and N-carbamoylputrescine amidohydrolase (Michael, 2016b, Michael, 2016a). Interestingly, plants (Bunsupa *et al.*, 2012, Lee & Cho, 2001) and some bacteria exemplified by *S. ruminantium* and *V. vulnificus* (Lee *et al.*, 2007, Takatsuka *et al.*, 2000) possess a bifunctional Odc/Ldc capable of synthesizing both Put and Cad. Spd is formed by spermidine synthase (SpdSyn) through aminopropylation of Put, using an aminopropyl group released by decarboxylation of S-adenosylmethionine (Michael, 2016a, Michael, 2016b). In addition, *E. coli* SpdSyn transforms Cad into aminopropyl-Cad, a Spd analogue sharing its growth stimulating properties (Kim *et al.*, 2016).

Two major structural protein super-families are responsible for polyamine biosynthesis through pyridoxal-5-phosphate (PLP)-dependent LAOdcs: the alanine racemase fold (AR-fold) super-family and the aspartate aminotransferase fold (AAT-fold) super-family (Eliot & Kirsch, 2004). Phylogenetic studies of the LAOdcs of the AR-fold super-family revealed that these

enzymes are widespread throughout the three domains of life (Lee *et al.*, 2007, Burrell *et al.*, 2010) while the AAT-fold LAOdcs are exclusive to Bacteria and Archaea. Bacterial AAT-fold LAOdcs can be divided in two types according to the presence or absence of a particular CheY-like response regulator receiver domain, known as the "wing domain", necessary for the formation of higher-order oligomers (Burrell *et al.*, 2010, Kanjee *et al.*, 2011b). The short form referred as wing-less LAOdc was found in *Firmicutes, Cyanobacteria* and *Actinobacteria* phyla, and a few "wing-less" AAT-fold decarboxylases from *Firmicutes* and *Actinobacteria* were shown to have an Adc activity, required in particular for biofilm formation in *Bacillus subtilis* (Burrell *et al.*, 2010). The long, wing domain-containing form appeared featured by *Proteobacteria* (Kanjee *et al.*, 2011b).

AAT-fold decarboxylases with the wing domain have been intensively studied in *Enterobacteria* since the early 1940s (Gale & Van Heyningen, 1942, Gale & Epps, 1944) because of the link between enterobacterial pathogenicity for humans and their capacity to withstand acid stress thanks to the crucial role of the inducible LAOdcs. Consequently, the current understanding of the AAT-fold LAOdc is based on analyses of a very limited number of bacterial species, *i.e.* mostly *Enterobacteria E. coli*, *Salmonella typhimurium*, *Vibrio cholerae* and *V. vulnificus*. At a specific acidic pH, expression of the decarboxylase gene is induced by an excess of the target amino acid uptaken by a dedicated inner membrane antiporter (Kanjee & Houry, 2013). The enzyme transforms the amino acid substrate into the corresponding polyamine upon consumption of a proton and production of a CO_2 molecule. In association with the polyamine excretion by the antiporter, this reaction results in an efficient buffering of the intracellular medium and the extracellular surroundings. These inducible stress response

116 decarboxylases are distinguished from "biosynthetic" enzymes that are involved only in
117 polyamine biosynthesis. *E. coli* encodes two biosynthetic decarboxylases (LdcC: Lys->Cad and
118 OdcC/SpeC: Orn->Put) responsible for Cad and Put biosynthesis respectively, and three acid
119 stress-inducible decarboxylases (LdcI: Lys->Cad, AdcI/AdiA: Arg->Agm and OdcI/SpeF: Orn->Put)
120 which together constitute a very robust acid stress response system that allows the bacterium
121 to survive upon acid stress as low as pH 2.0 (Zhao & Houry, 2010, Kanjee *et al.*, 2011a, Kanjee
122 & Houry, 2013). The importance of LdcI was also demonstrated in *S. typhimurium, V. cholerae*
123 and *V. vulnificus*, where it promotes growth and survival under acidic conditions but also
124 confers protection from oxidative stress insults (Merrell & Camilli, 2000, Kang *et al.*, 2007, Viala
125 *et al.*, 2011). It should be noted that LdcI-encoding genes are often designated as *cadA* as
126 originally proposed upon identification of this gene in *E. coli* (Tabor *et al.*, 1980).

127 *E. coli* LdcI but not LdcC interacts with the AAA+ ATPase RavA to assemble into a huge
128 macromolecular cage (Snider *et al.*, 2006, El Bakkouri *et al.*, 2010, Malet *et al.*, 2014, Kandiah *et*
129 *al.*, 2016). One of the functions of this mysterious complex is to protect LdcI from inhibition by
130 the stringent response alarmone ppGpp, thus enabling the bacterium to efficiently cope with
131 both acid and nutrient stress simultaneously (El Bakkouri *et al.*, 2010, Kanjee *et al.*, 2011a,
132 Malet *et al.*, 2014). While investigating why RavA binds only LdcI but not LdcC, we documented
133 numerous inconsistencies in annotation of enterobacterial *ldcI* and *ldcC* genes and realized that
134 each of these two families appeared to have a distinct genetic context (Kandiah *et al.*, 2016).
135 Thus, spurred on by the limited nature of the previous studies, we set out to perform an
136 extensive phylogenetic analysis of the AAT-fold LAOdcs in circa 4,500 complete prokaryotic
137 proteomes to decipher the evolutionary history of these proteins and their functional evolution.

138 In the present study, we revealed the ancestral nature of the wing-less LAOdcs in *Cyanobacteria*
139 and *Firmicutes*, and the complex evolutionary history of long AAT-fold LAOdcs in *Proteobacteria*,
140 leading to the emergence of distinct subfamilies. Moreover, we disclosed a novel subfamily of
141 enzymes, clearly distinct from the well-known LdcI, LdcC, AdcI, OdcI and OdcC families, but
142 more related to Ldc and Adc. Excitingly, this novel evolutionary subfamily has been overlooked
143 in previous phylogenetic analyses in spite of its wide distribution in *Betaproteobacteria* and
144 *Pseudomonadaceae*, implying that it deserves a thorough characterization and a functional
145 comparison with the known AAT-fold long LAOdc. The only previously mentioned LAOdc from
146 these taxa is the lysine decarboxylase LdcA from a major multidrug resistant opportunistic
147 human pathogen *Pseudomonas aeruginosa* (Chou *et al.*, 2010). Thus, here we went beyond the
148 initial characterization of the *P. aeruginosa* LdcA (Chou *et al.*, 2010), and further analyzed its
149 expression, regulation, and function in the light of the available knowledge in particular on *E.*
150 *coli* LdcI and LdcC. This combined phylogenetic and functional study revealed that LdcA belongs
151 to a novel subgroup of the long AAT-fold LAOdcs, and that its function is linked to Cad
152 production and to the general polyamine metabolism rather than to stress response.
153
154 **Results**
155 *Evolutionary history of bacterial LAOdcs*
156 An in-depth survey of 4,466 prokaryotic proteomes representing 1,904 species revealed 4,090
157 protein sequences belonging to the AAT-fold LAOdcs (13 of which were unannotated or
158 annotated as pseudo-genes) (Table S1). Representatives of this super-family are mainly present
159 in *Proteobacteria*, *Firmicutes*, *Actinobacteria* and *Cyanobacteria* (Fig. 1A). The corresponding

160 Maximum Likelihood (ML) tree could be divided in three parts (Fig. 1B). Cluster I encompasses
161 sequences devoid of the wing domain (short AAA-fold LAOdc), found in *Firmicutes*,
162 *Cyanobacteria* and *Actinobacteria* (Bootstrap value (BV) = 99%). Cluster II encloses nearly all
163 proteobacterial sequences and a few sequences from Firmicutes (BV = 99%), all containing a
164 wing domain. Cluster III branches in-between Cluster I and Cluster II; it is composed of a mix of
165 long and short AAT-fold LAOdc sequences from unrelated taxonomic groups (*Proteobacteria*,
166 *Actinobacteria*, *Bacteroidetes*, and *Firmicutes*), which strongly suggests that their taxonomic
167 distribution results from horizontal gene transfers among these lineages.

168 Within Cluster I, all cyanobacterial sequences group together albeit with a weak support
169 (Bootstrap value, BV < 90%) and appear widely distributed in this phylum (Fig. S1A).
170 Furthermore, the phylogeny of these sequences is overall consistent with a reference phylogeny
171 of *Cyanobacteria* based on ribosomal proteins (Fig. S1A and S1B). This indicates that a gene
172 coding for a wing-less AAT-fold LAOdc was ancestral and had been mainly transmitted vertically
173 in *Cyanobacteria*. Genomic context of LAOdc in Cyanobacteria is not conserved even in
174 relatively close species (Fig. S1C). Similarly, a large group of *Firmicutes* sequences is observed in
175 the tree (Fig. 1). Comparison of the taxonomic distribution and the phylogeny of these
176 sequences with a reference phylogeny of *Firmicutes* suggests the ancestral presence of a gene
177 coding for a short AAT-fold LAOdc in this phylum (Fig. S2A and S2B). Furthermore, most of
178 *Firmicutes* harbor two LAOdc copies (A and B) that can be distinguished by their genomic
179 context (Fig. S2C), with exception of the most early-branching lineages (a single copy in
180 *Natranaerobiaceae*, gene absence in *Halobacteroidaceae* and *Halanaerobiaceae*). The
181 paralogue A, ancestral in *Firmicutes*, presents a well-conserved genomic context (thymidylate

182 kinase and DNA polymerase III subunit delta). In contrast, the paralogue B appeared at the
183 emergence of *Clostridia* and *Bacilli,* likely as the result of a gene duplication event, and its
184 genetic context is not conserved. A loss of both paralogues can be inferred at the emergence of
185 *Lactobacillales* followed by a reacquisition in some *Streptococcaceae* and *Carnobacteriaceae* by
186 horizontal gene transfer from different *Firmicutes* donors (Fig. S2A). Finally, Cluster I
187 encompassed a group of sequences from *Actinobacteria*. These sequences emerged from the
188 *Firmicutes* group, suggesting that they have been acquired by horizontal gene transfer from
189 *Firmicutes*.

190 Analysis of proteobacterial LAOdcs composing the Cluster II of the tree revealed two
191 monophyletic groups, Odc (BV/Posterior probabilities PP = 100%/1) and LAdc (BV/PP = 100%/1)
192 (Fig. 2A and 2B). The LAdc group is further split into LdcI/LdcC (BV/PP = 100%/1), Adc (BV/PP =
193 93%/1), and a hitherto non-identified subfamily (BV/PP =100%/1), that will be referred as LdcA
194 in the name of its only previously mentioned member, LdcA from *P. aeruginosa* (Chou *et al.*,
195 2010). It should be emphasized that although the monophyly of OdcI/OdcC, LdcI/LdcC, Adc and
196 LdcA groups is well supported, the relationships between LdcI/LdcC, Adc and LdcA are
197 unresolved (BV/PP < 80%/0.67).

198 Comparison of LAOdc phylogeny, taxonomic distribution and genomic contexts with a
199 reference phylogeny of *Proteobacteria* suggests that OdcI could be ancestral in
200 *Bradyrhizobiaceae*, *Xanthobacteriaceae*, *Methylobacteriaceae* and *Beijerinckiaceae*
201 (*Alphaproteobacteria*) and *Vibrionaceae*, *Pasteurellaceae* and *Enterobacteriaceae*
202 (*Gammaproteobacteria*) (Fig. 3A). Interestingly, a few horizontal gene transfers of *odcI* occurred
203 from *Proteobacteria* to *Firmicutes*, especially to some *Lactobacillus, Staphylococcus lugdunensis*

204 and *Megasphaera elsdenii.* In contrast, *odcC* seems more recent and appears to result from a
205 gene duplication of *odcI* that occurred in *Enterobacteriaceae*, before the divergence of *Sodalis*
206 (BV/PP = 75%/1, Fig. 3B). Genes coding for OdcI and OdcC are clearly distinguished by their
207 context (Fig. 4). More precisely, *odcI* is predominantly upstream from a gene (*potE*) coding for
208 putrescine-ornithine antiporter, consistently with the function of OdcI that converts Orn to Put.
209 In contrast, OdcC coding gene is located in the vicinity of Fe^{2+}-trafficking protein (*yggX*) and a
210 lytic murein transglycosylase (*mltC*) genes.

211 LdcI appears to be ancestral in some gammaproteobacterial lineages (*Francisellaceae*,
212 *Aeromonadaceae*, *Vibrionaceae* and *Enterobacteriaceae*, Fig. 3A). Moreover, similar to
213 *odcI*/*odcC*, *ldcC* apparently derived from *ldcI*, and more precisely from a gene duplication that
214 occurred, as for *odcI*, just before the emergence of *Sodalis* (BV/PP = 100%/1, Figure 3B). The *ldcI*
215 gene, also called *cadA*, forms a *cadBA* operon together with the lysine-cadaverine antiporter-
216 encoding the *cadB* gene. In *Enterobacteriaceae*, this operon is known to be regulated by the
217 transcriptional factor CadC integrating three external signals – low pH, high lysine and low Cad
218 levels (Kuper & Jung, 2005, Fritz *et al*., 2009). Our analysis confirmed the conserved genomic
219 organization of the *cadCBA* system (Fig. 4) (Zhao & Houry, 2010) allowing *Enterobacteria* to
220 face acid and oxidative stresses. The *ldcC* genomic context seems to be also strongly conserved
221 (Fig. 4) with genes coding for hydroxymyristol acyl carrier protein dehydratase, UDP-N-
222 acetylglucosamine acetyltransferase, tetraacyldisaccharide-1-P synthase, ribonuclease HII, DNA
223 polymerase III alpha subunit, and acetyl-CoA carboxylase 2C alpha subunit upstream and
224 putative lyase and tRNA(Ile)-lysidine synthetase genes downstream.

225 In sharp contrast with OdcI/OdcC and LdcI/LdcC, Adc group presents a patchy taxonomic

226 distribution and their relationships are at odds with species phylogeny, with sequences from
227 different classes of *Proteobacteria* being intermixed on the tree (Fig. 3). This indicates that the
228 Adc subfamily was heavily impacted by horizontal gene transfers. Accordingly, it cannot be
229 inferred as ancestral in any taxonomic group. The genomic context of *adc* is not conserved (Fig.
230 4), precluding identification of potential functional partners. Interestingly, the *Burkholderia* sp.
231 AIU 395 LAOdc that locates in the Adc group was shown to possess a lysine decarboxylase and
232 oxidase activity (Sugawara *et al.*, 2014).

233 As specified above, beside OdcI/C, LdcI/C and Adc, a fourth group of LAOdc sequences
234 emerged in the tree. This group contains LdcA from *P. aeruginosa,* shown to possess a lysine
235 decarboxylase activity (Chou *et al.*, 2010). Homologues of LdcA are found in other
236 representatives of *Pseudomonadaceae*, as well as in nearly all *Betaproteobacteria*. Both groups
237 of sequences are well separated on the tree and widely distributed in these two taxa, and the
238 relationships among betaproteobacterial sequences are globally in agreement with the species
239 taxonomy. This suggests that an LdcA homologue was present in the ancestor of
240 *Pseudomonadaceae* and in the ancestor of *Betaproteobacteria* and has been conserved along
241 the diversification of these two taxa. Worthy of note, *ldcA* was secondly lost in *Neisseriaceae*
242 and *Nitrosomonadaceae*. The genetic environment of *ldcA* is not conserved (Fig. 4). To our
243 knowledge, the only publication describing a member of the LdcA subfamily concerns *P.*
244 *aeruginosa*, a highly versatile bacterium that efficiently grows on arginine but not on lysine
245 (Fothergill & Guest, 1977, Rahman & Clarke, 1980). In this organism exhibiting tightly
246 interconnected lysine and arginine catabolism networks (Chou *et al.*, 2010, Madhuri Indurthi *et*
247 *al.*, 2016), the *PA1818* gene was identified as a part of the ArgR regulon upon growth on excess

248 arginine, but was surprisingly found to code for a lysine decarboxylase, and not for an arginine
249 decarboxylase as one would have logically supposed, and therefore called *ldcA* (Chou *et al.*,
250 2010, Madhuri Indurthi *et al.*, 2016). *P. aeruginosa* is a major cause of gram-negative infections,
251 especially in patients with compromised and weakened immune system. This opportunistic
252 pathogen is also a well-identified threat for patients suffering from Cystic Fibrosis (CF), because
253 the chronic respiratory infections associated to host inflammatory responses lead to pulmonary
254 tissue destruction and lung failure. The occurrence and persistence of *P. aeruginosa* in the CF
255 patients' lungs, whose secretions were shown to be acidified and to become oxidative, hints to
256 a possible role of LdcA in promoting bacterial fitness. Therefore, in the following sections, we
257 chose to deepen the present knowledge on expression, regulation and functional
258 characterization of *P. aeruginosa* LdcA.
259
260 ldcA *expression is growth-phase dependent*
261 To determine the role of the LdcA protein in *P. aeruginosa*, the prerequisite was to know when
262 the protein is produced by the bacterium and what are the mechanisms controlling its
263 production. Thus, we first analyzed the expression of its gene by creating a transcriptional
264 fusion between the *ldcA* promoter (*PldcA*) and the reporter *lacZ* gene. The fusion was then
265 integrated into the chromosome of PAO1 (see Materials and Methods for further details), the
266 first *P. aeruginosa* sequenced strain (Stover *et al.*, 2000) considered as a reference strain and
267 widely studied. We then measured the β-galactosidase activity of the PAO1::P_{ldcA}-*lacZ* strain
268 grown in a minimal medium P (MMP) containing glutamate as a carbon source and lysine or
269 arginine (20mM) as additives. Unlike lysine, arginine was able to induce the expression of *ldcA* in

270 PAO1::P_{ldcA}-*lacZ* (not shown), in agreement with published data identifying ArgR as a positive
271 regulator of *ldcA* expression in the PAO1 strain (Chou *et al.*, 2010, Lu *et al.*, 2004).
272 The pattern of *ldcA* expression was followed during the growth both in minimal and rich
273 media. In MMP medium supplemented with glutamate and arginine (MMP-GR), the β-
274 galactosidase activity increased slightly but continuously along the growth and reached a
275 maximum in the stationary phase (Fig. 5A). Expression of *ldcA* in LB rich medium followed the
276 same pattern of expression (Fig. 5B), that was paralleled by an increase in LdcA protein amount
277 assessed by western blot (not shown). The expression level obtained in LB was two-fold lower
278 that the one measured in MMP-GR. Addition of 20 mM arginine to LB did not change the growth
279 rate of the bacteria but the *ldcA* promoter activity increased during the transition to the
280 stationary phase to reach a level similar to the one measured in MMP-GR (Fig. 5B), indicating a
281 probable limiting concentration of the amino acid in LB at late growth.
282
283 ldcA *expression differs from that of* ldcC *and* ldcI
284 The *ldcA* genomic context being different from that of *ldcI* and *ldcC* genes (Fig. 4), we wondered
285 if *ldcA* was also regulated differently than these genes; this knowledge could further provide
286 information on its role in *P. aeruginosa* physiology. Even if *E. coli* LdcC is called "constitutive
287 Lysine Decarboxylase", the corresponding gene was shown to be induced in stationary phase in
288 LB medium by RpoS, the sigma factor of stationary phase (Kikuchi *et al.*, 1998). However, *ldcA*
289 expression was not affected in a *rpoS* mutant background (data not shown), in agreement with
290 previous transcriptomics analyses demonstrating that *ldcA* is not part of the RpoS
291 regulon(Schuster *et al.*, 2004). To compare with LdcI, the "inducible Lysine Decarboxylase",

292 despite the absence of a CadC homologue in *P. aeruginosa,* we assessed if acid stress could
293 activate the expression of *ldcA* in a CadC-independent manner. Hence, we induced acid stress
294 by decreasing the pH of the medium to a value of 5 during the exponential phase of growth and
295 documented an absence of effect of this treatment on *ldcA* expression (Fig. S4A). In addition,
296 *ldcI* from *V. vulnificus* was reported to be induced by SoxR upon H_2O_2 stress (Kim *et al.*, 2006).
297 In *P. aeruginosa*, SoxR is not a key player in the oxidative stress response, but H_2O_2 activates the
298 global regulator OxyR that orchestrates the defense against ROS (Ochsner *et al.*, 2000). Yet,
299 addition of 1 mM of H_2O_2 in the culture did not affect *ldcA* expression (Fig. S4A). To conclude, *P.*
300 *aeruginosa* does not overexpress *ldcA* to respond to low pH or oxidative stress conditions.
301
302 *Low pH survival is not affected in absence of LdcA*
303 To clarify the function of LdcA in *P. aeruginosa,* a mutant deleted of the *ldcA* gene, as well as a
304 complemented strain in which one copy of *ldcA* driven by its own promoter was inserted in the
305 chromosome, were engineered (see Materials and Methods). Using Biolog system, a Phenotype
306 MicroArray analysis was carried out to test a large number of stress conditions in systematical
307 and reproducible manner. A potential role of LdcA in detoxifying and protecting *P. aeruginosa*
308 during acid, alkaline and oxidative stress, antibiotic treatment and toxic molecules causing DNA
309 damage, nitrosative stress, and membrane destabilization was assessed. After monitoring the
310 growth of *P. aeruginosa* in the different conditions in minimal medium during 24 hours (see
311 Materials and Methods), the "Area Under the Curve" (AUC) in each condition was calculated
312 and compared between the strains. Analysis of the growth fitness of wild-type, mutant and
313 complemented strains indicated that *P. aeruginosa* could grow optimally in a pH range from 5 to

314 10 without considerable effect on the metabolism and biomass growth. At pH 4 to 5, the
315 bacterial growth started to be strongly inhibited and the strains were unable to grow below pH
316 4 (Fig. S4B). This set of experiments did not show any significant difference between the mutant
317 and the wild-type and complemented strains, pointing to a non-involvement of LdcA in survival
318 at low pH. Similarly, no significant effect of *ldcA* absence on resistance against antibiotics,
319 oxidative and toxic agents could be detected (not shown). Hence LdcA seems not to be
320 important for any stress response.
321
322 *The Cad pool generated by LdcA impacts persistence phenotype and polyamine content*
323 In our quest for deciphering the importance of LdcA in bacterial physiology, we analyzed the
324 role of its product Cad shown to play a fundamental role in *P. aeruginosa* virulence. Indeed, this
325 polyamine was reported to be involved in the persistence of the bacterium which is of
326 importance for its eradication by antibiotics; specifically, Cad production was shown to lead to a
327 reduction of the dormant cells that form an antibiotic-tolerant subpopulation in MH medium
328 (Manuel *et al.*, 2010).
329 Therefore, to assess the role of LdcA in persistence, we first confirmed the impact of *ldcA*
330 mutation on Cad production in this rich MH medium. To do so, we quantified the intracellular
331 Cad amounts in the bacterial strains by liquid chromatography coupled to high resolution mass
332 spectrometry (LC/HRMS) during early-, mid- and late-exponential growth phases. Cad was
333 completely absent in the *ldcA* mutant and complementation with a wild-type *ldcA* copy restored
334 the metabolite level in the strain, indicating that, in PAO1, this polyamine is produced
335 exclusively through the enzymatic activity of LdcA in this growth condition (Fig. 6). Moreover,

336 the wild-type strain showed an impressive increase (around 25-fold) of Cad concentration
337 during the growth, probably reflecting the *ldcA* expression pattern in rich medium (increase
338 during exponential growth, Fig. 5B).

339 Then, the impact of *ldcA* on the number of persisters during carbenicillin treatment was
340 assessed. As anticipated, *ldcA* mutant showed a number of persisters significantly higher
341 compared to the wild-type PAO1 and complemented strains (Fig. S5), confirming the
342 importance of LdcA activity in the persistence phenotype.

343 Interestingly, in parallel to Cad, we also quantified the intracellular concentrations of two
344 other polyamines, Put and Spd, in the wild-type strain and *ldcA* mutant (Fig. 6). While in the
345 wild-type PAO1, the amount of Cad is clearly growth-phase dependent, the amounts of Put and
346 Spd were found to be abundant and constant in the MH medium. Remarkably, inactivation of
347 *ldcA* affected not only the production of Cad but also the amount of intracellular Put and Spd
348 which were reduced by around two-fold in the *ldcA* mutant at late exponential growth. This
349 could either indicate a higher turnover of polyamine metabolism in the *ldcA* mutant or a
350 reduced production of Put and Spd as a compensation for the absence of Cad.

351

352 *Polyamines are important for growth fitness*

353 As mentioned above, LdcA synthesis is induced in minimal MMP medium in presence of
354 arginine. Therefore, we monitored the growth of the *ldcA* mutant in this condition in presence
355 of either lysine, the substrate of LdcA, or Cad, the product of its enzymatic transformation. The
356 observed clear reduction of growth of the *ldcA* mutant highlighted the metabolic role of the
357 enzyme, whereas wild-type growth was restored in the complemented strain (Fig. 7A). Addition

358 of exogenous Cad was sufficient to restore a normal growth in the mutant indicating that the
359 limiting factor was indeed the polyamine product (Fig. 7B). Strikingly, growth was also restored
360 when Put (Fig. 7C) or Spd (Fig. 7D) were added to the growth medium at the same
361 concentrations, indicating that these polyamines can substitute for Cad as a growth factor.
362
363 **Discussion**
364 The present exhaustive phylogenetic analysis of the AAT-fold LAOdcs super-family
365 reveals that wing-less enzymes were ancestral in *Firmicutes*, in agreement with earlier reports
366 (Sekowska *et al.*, 1998, Burrell *et al.*, 2010). This analysis highlights also the ancestral presence
367 of wing-less AAT-fold LAOdc in *Cyanobacteria*. Yet, no LAOdc activity of a cyanobacterial AAT-
368 fold enzyme has been documented despite their purification from *Anabaena variabilis* and
369 *Nostoc punctiforme* (Burrell *et al.*, 2010). We show that wing domain-containing AAT-fold LAOdc
370 emerged during the diversification of *Proteobacteria*, suggesting that short AAT-fold LAOdc
371 could be more ancient and that the acquisition of the CheY-like wing domain occurred likely
372 secondarily, as previously proposed (Burrell *et al.*, 2010, Kanjee *et al.*, 2011a). The absence of
373 AR-fold decarboxylases in *Firmicutes* implies that their AAT-fold decarboxylases would be the
374 only route for polyamine biosynthesis and thus emphasizes the importance of these enzymes in
375 this phylum. The *Firmicutes* AAT-fold LAOdc correspond to two paralogues (A and B) present in
376 most species and easily distinguishable by their genomic context. These two copies result from a
377 duplication event that occurred very early during diversification of the phylum, probably in the
378 ancestor of Clostridia and Bacilli (Fig. S1). Paralogue A encompasses the *B. subtilis yaaO*
379 (Sekowska *et al.*, 1998), while paralogue B contains the *B. subtilis speA* gene coding for an

380 arginine decarboxylase (NP_389346.1) (Burrell *et al.*, 2010). Two other *Firmicutes* proteins
381 corresponding to paralogue B sequences (from *Clostridium difficile* YP_001087362.1 and *S.*
382 *ruminantium* WP_014425426.1) (Fig. S2B) were also shown to possess an arginine
383 decarboxylase activity (Burrell *et al.*, 2010, Liao *et al.*, 2008), which led to a hypothesis that
384 paralogue B AAT-fold decarboxylases would be Adcs (Burrell *et al.*, 2010). The function of
385 paralogue A awaits further investigation and, to our knowledge, the only study focused on the
386 *yaaO* gene (paralogue A) concluded that in *B. subtilis* this protein had no effect on polyamine
387 production (Sekowska *et al.*, 1998).

388 Regarding the evolutionary history of the wing domain-containing LAOdcs, our analysis
389 reveals that proteobacterial LAOdcs form two monophyletic groups, Odc and LAdc. Thus, lysine
390 and arginine decarboxylases appear more closely related to each other than to ornithine
391 decarboxylases, although the relationships among the two Ldc families (LdcI/C and LdcA) and
392 the Adc family are not resolved (PP <0.5) (Fig. 2B). Furthermore, we showed that the
393 proteobacterial biosynthetic OdcC and LdcC emerged from inducible Odc and Ldc (*i.e.* OdcI and
394 LcdI, respectively) through two independent gene duplication events that occurred in
395 *Enterobacteriaceae*, after the divergence of *Sodalis*. Given that both duplication events seem to
396 occur in the same branch of the phylogenetic tree, it is tempting to hypothesize that they are
397 linked, and that a functional connection between both biosynthetic subgroups may have
398 existed. The emergence of biosynthetic enzymes from inducible ones may appear contra-
399 intuitive at the first glance, but may reflect an expansion and a diversification of polyamine
400 functions in these lineages. This would also explain why *Enterobacteriaceae* possess also a
401 constitutive pathway of polyamine synthesis through an AR-fold Adc.

402 The exhaustive phylogenetic analysis of AAT-fold decarboxylases discloses multiple cases
403 of horizontal gene transfers (e.g. within Cluster III, from *Firmicutes* to *Firmicutes* and to
404 *Actinobacteria* within Cluster I, but also from *Proteobacteria* to *Firmicutes* within cluster II).
405 Interestingly, the two wing-less AAT-fold LAOdc coding genes found in *L. saerimneri* 30a were
406 proposed to result from the horizontal gene transfer of an acid stress inducible Odc from
407 *Enterobacteriaceae*, followed by a gene duplication event (Romano *et al.*, 2013, Romano *et al.*,
408 2014). One of the two resulting paralogues is thought to have kept the original function
409 (WP_009553942.1), while the other acquired the capacity to use lysine as substrate
410 (EKW98991.1). Instead, our analysis points to a different scenario. In fact, the two copies
411 present in *L. saerimneri* branch in two different parts of the OdcI tree (Fig. S3), meaning that
412 they have different origins, and result likely from two independent horizontal gene transfer
413 events of OdcI coding genes, whereupon one of these two acquired genes shifted secondarily
414 towards the capacity to use lysine instead of ornithine. Interestingly, the lysine decarboxylating
415 copy is present in various *Lactobacilli*, while the copy using ornithine as substrate is specific to *L.*
416 *saerimneri* (Fig. S3), suggesting that the former was acquired first. Remarkably, these two
417 enzymes rely on the same antiporter capable to exchange both ornithine/Put and lysine/Cad
418 pairs, resulting in a unique three-component decarboxylation system involved in acid stress
419 response {Romano, 2013 #52}. This case of substrate specificity shift is probably not an
420 exception, as exemplified by *Burkholderia* sp. AIU 395 in which an AAT-fold enzyme using lysine
421 as substrate branches within the Adc cluster in phylogenetic trees (Fig. 2A). Beside substrate
422 shift, existence of dual specificity has been most extensively documented in the case of AR-fold
423 LOdcs, exemplified by bifunctional enzymes of *S. ruminantium* (Takatsuka *et al.*, 2000) and *V.*

424 *vulnificus* (Lee *et al.*, 2007). In particular, crystal structures of the *V. vulnificus* enzyme in
425 complex with either Put or Cad revealed that the dual substrate specificity is based on a bridging
426 water molecule necessary for the binding of a shorter Put ligand in addition to the longer Cad. A
427 similar dual substrate specificity mechanism may also exist in the case of the AAT-fold LAOdc
428 enzymes although it has not been documented up to now.

429 Altogether, our data indicate that functional changes affecting gene regulation, substrate
430 fixation, and cellular function occurred several times during the evolution of AAT-fold enzymes.
431 In the light of these observations, one may wonder if the so-called Adc, LdcC, LdcI, OdcC, and
432 OdcI clusters defined according to phylogenetic criteria correspond indeed to homogeneous
433 functional groups and thus if phylogenetic criteria/sequence similarity based measures are good
434 predictors of the function of the AAT-fold enzymes. The very restricted number of
435 experimentally characterized enzymes calls for caution and for the urgent need for additional
436 experimental data.

437 One of the main results of the presented phylogenetic analysis is the identification of a
438 novel large family of decarboxylases, called LdcA, ancestral in *Betaproteobacteria* and
439 *Pseudomonadaceae*. Thus, the second part of this work was dedicated to functional
440 characterization of the LdcA from a major human opportunistic pathogen *P. aeruginosa*.

441 The *ldcA* gene belongs to the core genome of *P. aeruginosa*, comprising at least 4,000
442 conserved genes (Hilker *et al.*, 2015, Valot *et al.*, 2015). Similarly to *ldcI*, in *P. aeruginosa,*
443 *Pseudomonas resinovorans, Pseudomonas denitrificans* and *Pseudomonas knackmusii, ldcA* is
444 organized in a gene cluster with a gene coding for a homologue of the CadB antiporter,
445 although *cadB* (*PA1819* in *P. aeruginosa*) appears downstream, and not upstream, of the lysine

446 decarboxylase-encoding gene. The presence of a dedicated Lys/Cad transporter could be
447 important from a physiological standpoint because CadB is involved not only in
448 substrate/product exchange but also in the generation of proton motive force
449 (Soksawatmaekhin *et al.*, 2004). Remarkably, the proximity of *cadB* and *ldcA* is an exception in
450 the *ldcA* subfamily (Fig. 4), which does not rule out a hypothesis that LdcA could have another
451 function in other taxa. The whole of our data suggests that LdcI and *P. aeruginosa* LdcA are
452 different in terms of regulation and function. Indeed, we clearly show that LdcA is not evolved
453 for acid or oxidative stress response, and its expression is triggered by neither of these stresses;
454 instead it is controlled by ArgR and QS. More similar to LdcC, *P. aeruginosa* LdcA, and certainly
455 the other members of this novel lysine decarboxylase subfamily, are biosynthetic enzymes
456 responsible for the Cad production by the bacterium.

457 Importantly, LdcA is the only Cad producing enzyme in *P. aeruginosa* PAO1, as
458 demonstrated by the measurement of the intracellular contents of Cad (Fig. 6). This conclusion
459 was unexpected considering that the product of another gene, *PA4115*, was previously reported
460 to be responsible for 25% of Cad production in overnight cultures grown in the same medium as
461 the one used in our assays, and therefore proposed to be an Ldc (Manuel *et al.*, 2010). After
462 carboxypenicillin treatment, the *PA4115* mutant exhibited an increased number of persisters
463 that was significantly reduced upon addition of exogenous Cad, further supporting the
464 hypothesis of PA4115 being an Ldc (Manuel *et al.*, 2010). Yet, our careful inspection of its
465 sequence revealed that PA4115 belongs to the family of Lonely Guy (LOG) proteins because it
466 contains a highly conserved PGGxGTxxE motif and a nucleotide-binding Rossmann fold.
467 Remarkably, LOG proteins were shown to be often mis-annotated as lysine decarboxylase

468 enzymes, yet without support by biochemical or functional data, whereas they actually possess
469 a cytokinin-specific phosphoribohydrolase activity (Dzurova *et al.*, 2015, Seo & Kim, 2017) or a
470 pyrimidine/purine nucleotide 5'-monophosphate nucleosidase activity (Sevin *et al.*, 2017).
471 Recently, PPnN (or YghD) from *E. coli*, a close homologue sharing 56% identity with PA4115, has
472 been shown to catalyze the hydrolysis of N-glycosidic bond of AMP, GMP, IMP, CMP, dTMP and
473 UMP to form ribose 5-phosphate and the corresponding free base. Hence, it is quite likely that
474 PA4115 catalyzes the same reaction and plays a role in maintaining the nucleotide pool
475 homeostasis by degrading excess nucleotides in *P. aeruginosa* (Sevin *et al.*, 2017). Therefore,
476 the reduced production of Cad in *PA4115* mutant needs to be confirmed because the
477 relationship between PA4115 and LdcA activity is not clear and could involve indirect causes.

478 The persistence phenotype observed in *ldcA* mutants is consistent with the beneficial
479 effect of LdcA on growth fitness. Indeed, recent research on bacterial persistence uncovered
480 intracellular ATP concentrations as being one of the major factors affecting the amount of
481 persister cells, and demonstrated that ATP levels are sufficient to predict bacterial tolerance to
482 antibiotics (Conlon *et al.*, 2016, Shan *et al.*, 2017). Considering that Cad produced by LdcA is
483 metabolized and used up by the Krebs cycle to create ATP and that the activity of the lysine/Cad
484 antiporter generates proton motive force essential for ATP synthesis (Soksawatmaekhin *et al.*,
485 2004), one would expect that in *P. aeruginosa* the *ldcA* mutation may lead to a decrease in ATP
486 levels, which in turn would result in an increase of persisters' population. This hypothesis could
487 be challenged by blocking the Cad degradation pathway or the CadB antiporter activity.

488 The capacity of Put and Spd to complement the growth phenotype of the *ldcA* mutant
489 and boost *P. aeruginosa* cultures in minimal medium suggests that in *P. aeruginosa* the three

490 major polyamines share certain properties. In the same lines, Cad was shown to substitute for
491 Put and Spd as growth factors in *E. coli* cells depleted of these two polyamines (Igarashi *et al.*,
492 1986). The growth phenotype described in our work is observed under specific growth
493 conditions. It reveals the importance of Cad when growing *P. aeruginosa* in minimal medium
494 and highlights a certain redundancy in the function of polyamines. It remains to be investigated
495 whether the phenotype is linked to a regulatory effect of Cad or to its anabolism. Recent
496 literature about *Eikenella corrodens* has pointed out the importance of an AAT-fold Ldc
497 (belonging to LdcI group) as a virulence factor against eukaryotic cells that acts through
498 depletion of essential lysine (Lohinai *et al.*, 2015). Therefore the potential role of LdcA in the
499 virulence of *P. aeruginosa* may warrant further investigation. In the present study, we observed
500 that the absence of the enzyme did not affect T3SS-dependent cytotoxicity or the mobility
501 relying on flagellum and Type IV pili (not shown). However, it would also be relevant to probe
502 the importance of LdcA during mouse infection, where the proper functioning of *P. aeruginosa*
503 metabolism is primordial for virulence.

504 Our study reveals that the *ldcA* gene is relatively ancient in *Proteobacteria*, being
505 ancestral in *Betaproteobacteria* and in *Pseudomonadaceae*, two taxa that cover a wide range of
506 ecological niches. Information about regulation and function of an enzyme of the previously
507 unknown LdcA subfamily enables a step further towards understanding of the evolution and the
508 importance of Cad metabolism in bacteria.

509

510 **Experimental procedures**

511

Phylogeny: Dataset assembly

Functionally characterized sequences of AAT-fold LAOdcs were retrieved from NCBI: LdcI (NP_418555.1), LdcC (NP_414728.1), Adc (NP_418541.1), OdcC (NP_417440.1), and OdcI (NP_415220.1) from *E. coli* str. K-12 substr., MG1655 and LdcA (NP_250509.1) from *P. aeruginosa* PAO1. These sequences were used as seeds to query a local database containing 4,466 complete proteomes of prokaryotes downloaded from the NCBI (ftp://ftp.ncbi.nlm.nih.gov) with the BLASTP 2.2.6 software (Altschul *et al.*, 1997) using default parameters. Homologues of LAODc were retrieved and aligned using MAFFT v7 (Katoh & Standley, 2013). The resulting multiple alignment was used to build a HMM profile with the HMMbuild program from the HMMER v3.1b1 package (McClure MA, 1996). This profile was then used to query the local database of complete proteomes with the HMMsearch program. Sequences with e-values lower than 2.2e-13 were retrieved. Finally, the search for potential unannotated sequences was performed using TBLASTN 2.2.6 on genomic sequences corresponding to the 4,466 complete proteomes. This led to the identification of 4,090 homologous sequences.

Phylogeny: Phylogenetic inference

To limit taxonomic redundancy for phylogenetic analysis, a sampling of the retrieved sequences by selecting randomly one strain per species has been performed. Multiple alignments were built with MAFFT using the L-INS-i option that allows the construction of accurate multiple alignments and trimmed with BMGE v1.1 with matrix substitution BLOSUM30 (Criscuolo & Gribaldo, 2010).

534 Maximum likelihood trees were inferred with PhyML 3.1 (Guindon *et al.*, 2010). The best
535 suited evolutionary models were selected using the model test tool implemented in IQ-TREE
536 v1.4.1 according to the BIC criteria (Nguyen *et al.*, 2015). The robustness of the inferred trees
537 was assessed using the non-parametric procedure implemented in PhyML (100 replicates of the
538 original datasets). Bayesian trees were inferred using MrBayes v3.2.6 (Ronquist & Huelsenbeck,
539 2003). Two runs were launched with four chains for each run (50,000 iterations). The first 25%
540 of the trees were discarded as burn-in and chain convergence has been checked by analysing
541 the evolution of the Ln(L) curve and checking the average standard deviation of split frequencies
542 values. Figures of trees have been generated using EvolView (He *et al.*, 2016)
543 (http://nar.oxfordjournals.org/content/44/W1/W236) and iTOL (Letunic & Bork, 2016).
544 Genomic context figures have been generated using GeneSpy (https://lbbe.univ-
545 lyon1.fr/GeneSpy/).
546 Reference phylogenies of species containing Ldc, Adc or Odc homologues were inferred
547 using ribosomal proteins as suggested elsewhere (Ramulu *et al.*, 2014). Ribosomal protein
548 sequences from the complete proteomes of these species were identified using the RiboDB
549 database engine (Jauffrit *et al.*, 2016) and aligned with MAFFT using the L-INS-i option. The
550 resulting multiple alignments were trimmed as described above and combined to build a large
551 supermatrix that was used to build maximum likelihood phylogenetic trees.
552
553 *Bacterial strains, plasmids, and growth conditions*
554 The bacterial strains and plasmids used in this study are listed in Table S2 in the supplemental
555 material. Bacteria were cultivated aerobically at 37°C in rich Lysogeny Broth (LB) medium, in

556 Mueller Hinton II (Becton Dickinson) or in minimal medium P (30mM Na_2HPO_4, 14 mM KH_2PO_4,
557 20mM $(NH4)_2SO_4$, 1 mM $MgSO_4$, 4µM $FeSO_4$, 0.4 µM Pyridoxal-5'-phosphate, pH 7.4) (Haas *et*
558 *al.*, 1977) containing the indicated carbon and nitrogen sources. *P. aeruginosa* was also cultured
559 on Pseudomonas Isolation Agar plates (PIA; Difco). When required, antibiotics were added at
560 the following concentrations (in µg/ml): 100 (ampicillin), 25 (gentamycin), 25 (kanamycin) and
561 10 (tetracycline) for *E. coli*, 200 (carbenicillin), 200 (gentamycin) and 200 (tetracycline) for *P.*
562 *aeruginosa.*
563
564 *Genetic manipulations*
565 To delete *ldcA* gene, fused uspstream and downstream flanking regions of the gene were
566 generated by "Splicing by Overlap Extension" (SOE)-PCR using PAO1 genomic DNA as matrix and
567 appropriate primer pairs. The resulting fragment of 819 bp was cloned into pCR-Blunt II-TOPO
568 vector, sequenced and then subcloned into *Bam*HI-*Hin*dIII sites of pEXG2, leading to
569 pEXG2Δ*ldcA.* The suicide plasmid carries the counter-selectable *sacB* marker from *B. subtilis*
570 which confers sensitivity to sucrose. The plasmid was mobilized into *P. aeruginosa* strain by
571 triparental mating, using the conjugative properties of the helper plasmid pRK2013. Co-
572 integration events were selected on PIA plates containing gentamycin. Single colonies were then
573 plated on PIA medium containing 5% (w/v) sucrose to select for the loss of plasmid: the
574 resulting sucrose-resistant strains were checked for antibiotic sensitivity and for *ldcA* (wild-type
575 or truncated gene) genotype by PCR.
576 To complement the *ldcA* mutant, a 2785 bp-long fragment encompassing the coding
577 sequence and 495 bases upstream the ATG was PCR amplified from PAO1 genomic DNA using

578 appropriate primer pairs. The PCR product was cloned into pCR-Blunt II-TOPO and sequenced.
579 The *Spe*I restriction fragment was subcloned in mini-CTX1 cut with the same enzyme, leading to
580 miniCTX-*ldcA*. A mini-CTX derivative was used to construct a *lacZ* reporter vector. PCR
581 amplification was used to produce the 548 bp-long *ldcA* promoter fragment (-498/+44 relative
582 to translation initiation) with appropriate primers. After ligation into pCR-Blunt II-TOPO vector
583 and sequencing, the fragment was sub-cloned into the *Xho*I-*Eco*RI sites of mini-CTX-lacZ. Both
584 miniCTX-*ldcA* and mini-CTX-*PldcA-lacZ* were introduced into *P. aeruginosa* by triparental
585 conjugation and the transconjugants were selected on PIA plates containing tetracycline. The
586 pFLP2 plasmid was then used to excise the FRT cassette as described (Hoang *et al.*, 1998).
587 Plasmids and primers used in PCR are listed in the Tables S2 and S3, respectively.
588
589 *β-Galactosidase assays*
590 Bacteria were grown aerobically at 37°C in 100 ml flasks with agitation (300 rpm). At the
591 indicated OD, β-galactosidase activity was assayed as described (Miller, 1972), with details
592 reported in (Thibault *et al.*, 2009).
593
594 *Intracellular metabolite analysis*
595 Strains were first isolated from an overnight solid culture at 37°C on Mueller Hinton II agar 1.5%.
596 Precultures and cultures were performed on a Minitron II rotary shaker at 220 rpm (Infors HT)
597 under aerobic conditions (10% of total volume of Erlenmeyer flask). A few bacterial colonies
598 from the agar plate were precultured overnight at 37°C and an aliquot was withdrawn and
599 diluted to an OD_{600} of ~0.1 in a fresh culture medium for the culture step. Growth curves were

600 determined for each strain and used to determine their respective concentration (CFU/ml) and
601 the OD at which the bacteria should be harvested to correspond to early-, mid-, and late-
602 exponential phases.

603 The protocol of the intracellular metabolites sampling was adapted from a previously
604 described procedure (Aros-Calt *et al.*, 2015). In brief, a 5 ml aliquot of cell culture broth was
605 taken from the main culture and was filtered in a few seconds using poly(ether sulfone) sterile
606 membrane disc filters (Supor450, 0.45 µm pore size, PALL) mounted on a Millipore filtration
607 device (Darmstadt). The bacteria on the filter were quickly washed with 5 ml of 0.6% NaCl
608 solution maintained at room temperature. The filter was then rapidly transferred to a 50 ml
609 Falcon tube containing 5 ml of cold 60% ethanol (v/v, ≤ −20°C). The Falcon tube was
610 subsequently quickly immersed in liquid nitrogen. Following this quenching step, tubes
611 containing bacteria on filters in the extraction solution were vortexed 10 times on ice to remove
612 the cells from the filter. Then, a 1 ml aliquot of the cell suspension was transferred to 2 ml tubes
613 containing 0.1 mm glass beads (Bertin Technologies). Cell disruption was performed by three
614 cycles in a Precellys 24 homogenizer (Bertin Technologies) for 30 s at 3,800 rpm at ~4°C. The
615 glass beads and cell debris were separated from the supernatant by centrifugation for 5 min at
616 4°C and 10,000g. A 400 µL aliquot of the supernatant was withdrawn and further vacuum-dried
617 using a SpeedVac instrument (Thermo Fisher Scientific) and stored at −80°C until analysis. Dried
618 extracts were dissolved in an adjusted volume of 95% mobile phase A / 5% mobile phase B to
619 obtain the equivalent of 1.25 10^7 CFU in 15µl before analysis by LC/HR-MS.

620 To detect intracellular metabolites, LC/HR-MS experiments were performed using a Dionex
621 Ultimate chromatographic system (Thermo Fisher Scientific) coupled to an Exactive (Orbitrap)

622 mass spectrometer from Thermo Fisher Scientific fitted with an electrospray source. The mass
623 spectrometer was externally calibrated before each analysis using the manufacturer's
624 predefined methods and recommended calibration mixture provided by the manufacturer.
625 Chromatographic separation was performed on a Discovery HS F5 PFPP 5 µm, 2.1 × 250 mm
626 column (Sigma) at 30°C. The chromatographic system was equipped with an on-line pre-filter
627 (Thermo Fisher Scientifics). Mobile phases were 100% water (A) and 100% ACN (B), both of
628 which containing 0.1% formic acid. Chromatographic elution was achieved with a flow rate of
629 250 µl/min. After injection 15 µl of sample, elution started with an isocratic step of 2 min at 5%
630 phase B, followed by a linear gradient from 5 to 100% of phase B in 18 min. These proportions
631 were kept constant for 4 min before returning to 5% of phase B and letting the system
632 equilibrate for 6 min. The column effluent was directly introduced into the electrospray source
633 of the mass spectrometer, and analyses were performed in the positive ion mode. Source
634 parameters were as follows: capillary voltage set at 5 kV; capillary temperature at 300°C; sheath
635 and auxiliary gas (nitrogen) flow rates at 50 and 25 arbitrary units, respectively; mass resolution
636 power of the analyzer set at 50,000 at m/z 200 (full width at half maximum, FWHM) for singly
637 charged ions. The acquisition was achieved from m/z 50 to 250 in the positive ionization mode
638 during the first 12 min of the run. Under these conditions were achieved a good separation and
639 detection (with an average mass accuracy better than 3ppm) of the targeted molecules (under
640 their $[M+H]^+$ form). These species were readily identified in the extracts through the use of the
641 corresponding commercial molecules obtained from Sigma-Aldrich. Extracted ion
642 chromatograms were generated and resulting peaks integrated using the Xcalibur software
643 (version 2.1, Thermo Fisher Scientific) for Spd ($[M+H]^+$ at theoretical m/z 146.1652, retention

time 5.24 min), Put (m/z 89.1073, 3.63 min) and Cad (m/z 103.1230, 3.94 min).

REFERENCES

Altschul, S.F., T.L. Madden, A.A. Schaffer, J. Zhang, Z. Zhang, W. Miller & D.J. Lipman, (1997) Gapped BLAST and PSI-BLAST: a new generation of protein database search programs. *Nucleic Acids Res* **25**: 3389-3402.

Aros-Calt, S., B.H. Muller, S. Boudah, C. Ducruix, G. Gervasi, C. Junot & F. Fenaille, (2015) Annotation of the Staphylococcus aureus Metabolome Using Liquid Chromatography Coupled to High-Resolution Mass Spectrometry and Application to the Study of Methicillin Resistance. *J Proteome Res* **14**: 4863-4875.

Bunsupa, S., K. Katayama, E. Ikeura, A. Oikawa, K. Toyooka, K. Saito & M. Yamazaki, (2012) Lysine decarboxylase catalyzes the first step of quinolizidine alkaloid biosynthesis and coevolved with alkaloid production in leguminosae. *Plant Cell* **24**: 1202-1216.

Burrell, M., C.C. Hanfrey, L.N. Kinch, K.A. Elliott & A.J. Michael, (2012) Evolution of a novel lysine decarboxylase in siderophore biosynthesis. *Mol Microbiol* **86**: 485-499.

Burrell, M., C.C. Hanfrey, E.J. Murray, N.R. Stanley-Wall & A.J. Michael, (2010) Evolution and multiplicity of arginine decarboxylases in polyamine biosynthesis and essential role in Bacillus subtilis biofilm formation. *J Biol Chem* **285**: 39224-39238.

Chou, H.T., M. Hegazy & C.D. Lu, (2010) L-lysine catabolism is controlled by L-arginine and ArgR in Pseudomonas aeruginosa PAO1. *J Bacteriol* **192**: 5874-5880.

Conlon, B.P., S.E. Rowe, A.B. Gandt, A.S. Nuxoll, N.P. Donegan, E.A. Zalis, G. Clair, J.N. Adkins, A.L. Cheung & K. Lewis, (2016) Persister formation in Staphylococcus aureus is associated with ATP depletion. *Nat Microbiol* **1**: 16051.

Criscuolo, A. & S. Gribaldo, (2010) BMGE (Block Mapping and Gathering with Entropy): a new software for selection of phylogenetic informative regions from multiple sequence alignments. *BMC Evol Biol* **10**: 210.

Dela Vega, A.L. & A.H. Delcour, (1996) Polyamines decrease Escherichia coli outer membrane permeability. *J Bacteriol* **178**: 3715-3721.

Di Martino, M.L., R. Campilongo, M. Casalino, G. Micheli, B. Colonna & G. Prosseda, (2013) Polyamines: emerging players in bacteria-host interactions. *Int J Med Microbiol* **303**: 484-491.

Dzurova, L., F. Forneris, S. Savino, P. Galuszka, J. Vrabka & I. Frebort, (2015) The three-dimensional structure of "Lonely Guy" from Claviceps purpurea provides insights into the phosphoribohydrolase function of Rossmann fold-containing lysine decarboxylase-like proteins. *Proteins* **83**: 1539-1546.

El Bakkouri, M., I. Gutsche, U. Kanjee, B. Zhao, M. Yu, G. Goret, G. Schoehn, W.P. Burmeister & W.A. Houry, (2010) Structure of RavA MoxR AAA+ protein reveals the design principles of a molecular cage modulating the inducible lysine decarboxylase activity. *Proc Natl Acad Sci U S A* **107**: 22499-22504.

Eliot, A.C. & J.F. Kirsch, (2004) Pyridoxal phosphate enzymes: mechanistic, structural, and evolutionary considerations. *Annu Rev Biochem* **73**: 383-415.

Fothergill, J.C. & J.R. Guest, (1977) Catabolism of L-lysine by Pseudomonas aeruginosa. *J Gen Microbiol* **99**: 139-155.

Fritz, G., C. Koller, K. Burdack, L. Tetsch, I. Haneburger, K. Jung & U. Gerland, (2009) Induction kinetics of a conditional pH stress response system in Escherichia coli. *J Mol Biol* **393**: 272-286.

Gale, E.F. & H.M. Epps, (1944) Studies on bacterial amino-acid decarboxylases: 1. l(+)-lysine decarboxylase. *Biochem J* **38**: 232-242.

Gale, E.F. & W.E. Van Heyningen, (1942) The effect of the pH and the presence of glucose during growth on the production of alpha and theta toxins and hyaluronidase by Clostridium welchii. *Biochem J* **36**: 624-630.

Guindon, S., J.F. Dufayard, V. Lefort, M. Anisimova, W. Hordijk & O. Gascuel, (2010) New algorithms and methods to estimate maximum-likelihood phylogenies: assessing the performance of PhyML 3.0. *Syst Biol* **59**: 307-321.

Haas, D., B.W. Holloway, A. Schambock & T. Leisinger, (1977) The genetic organization of arginine biosynthesis in Pseudomonas aeruginosa. *Mol Gen Genet* **154**: 7-22.

Hilker, R., A. Munder, J. Klockgether, P.M. Losada, P. Chouvarine, N. Cramer, C.F. Davenport, S. Dethlefsen, S. Fischer, H. Peng, T. Schonfelder, O. Turk, L. Wiehlmann, F. Wolbeling, E. Gulbins, A. Goesmann & B. Tummler, (2015) Interclonal gradient of virulence in the Pseudomonas aeruginosa pangenome from disease and environment. *Environ Microbiol* **17**: 29-46.

Hoang, T.T., R.R. Karkhoff-Schweizer, A.J. Kutchma & H.P. Schweizer, (1998) A broad-host-range Flp-FRT recombination system for site-specific excision of chromosomally-located DNA sequences: application for isolation of unmarked Pseudomonas aeruginosa mutants. *Gene* **212**: 77-86.

Igarashi, K., (2006) [Physiological functions of polyamines and regulation of polyamine content in cells]. *Yakugaku Zasshi* **126**: 455-471.

Igarashi, K. & K. Kashiwagi, (2015) Modulation of protein synthesis by polyamines. *IUBMB Life* **67**: 160-169.

Igarashi, K., K. Kashiwagi, H. Hamasaki, A. Miura, T. Kakegawa, S. Hirose & S. Matsuzaki, (1986) Formation of a compensatory polyamine by Escherichia coli polyamine-requiring mutants during growth in the absence of polyamines. *J Bacteriol* **166**: 128-134.

Jauffrit, F., S. Penel, S. Delmotte, C. Rey, D.M. de Vienne, M. Gouy, J.P. Charrier, J.P. Flandrois & C. Brochier-Armanet, (2016) RiboDB Database: A Comprehensive Resource for Prokaryotic Systematics. *Mol Biol Evol* **33**: 2170-2172.

Kamio, Y. & K. Nakamura, (1987) Putrescine and cadaverine are constituents of peptidoglycan in Veillonella alcalescens and Veillonella parvula. *J Bacteriol* **169**: 2881-2884.

Kamio, Y., H. Poso, Y. Terawaki & L. Paulin, (1986) Cadaverine covalently linked to a peptidoglycan is an essential constituent of the peptidoglycan necessary for the normal growth in Selenomonas ruminantium. *J Biol Chem* **261**: 6585-6589.

Kandiah, E., D. Carriel, J. Perard, H. Malet, M. Bacia, K. Liu, S.W. Chan, W.A. Houry, S. Ollagnier de Choudens, S. Elsen & I. Gutsche, (2016) Structural insights into the Escherichia coli lysine decarboxylases and molecular determinants of interaction with the AAA+ ATPase RavA. *Sci Rep* **6**: 24601.

Kang, I.H., J.S. Kim, E.J. Kim & J.K. Lee, (2007) Cadaverine protects Vibrio vulnificus from superoxide stress. *J Microbiol Biotechnol* **17**: 176-179.

Kanjee, U., I. Gutsche, E. Alexopoulos, B. Zhao, M. El Bakkouri, G. Thibault, K. Liu, S. Ramachandran, J. Snider, E.F. Pai & W.A. Houry, (2011a) Linkage between the bacterial acid stress and stringent responses: the structure of the inducible lysine decarboxylase. *EMBO J* **30**: 931-944.

Kanjee, U., I. Gutsche, S. Ramachandran & W.A. Houry, (2011b) The enzymatic activities of the Escherichia coli basic aliphatic amino acid decarboxylases exhibit a pH zone of inhibition. *Biochemistry* **50**: 9388-9398.

Kanjee, U. & W.A. Houry, (2013) Mechanisms of acid resistance in Escherichia coli. *Annu Rev Microbiol* **67**: 65-81.

Karatan, E. & A.J. Michael, (2013) A wider role for polyamines in biofilm formation. *Biotechnol Lett* **35**: 1715-1717.

Katoh, K. & D.M. Standley, (2013) MAFFT multiple sequence alignment software version 7: improvements in performance and usability. *Mol Biol Evol* **30**: 772-780.

Kikuchi, Y., O. Kurahashi, T. Nagano & Y. Kamio, (1998) RpoS-dependent expression of the second lysine decarboxylase gene in Escherichia coli. *Biosci Biotechnol Biochem* **62**: 1267-1270.

Kim, J.S., S.H. Choi & J.K. Lee, (2006) Lysine decarboxylase expression by Vibrio vulnificus is induced by SoxR in response to superoxide stress. *J Bacteriol* **188**: 8586-8592.

Kim, S.H., Y. Wang, M. Khomutov, A. Khomutov, C. Fuqua & A.J. Michael, (2016) The Essential Role of Spermidine in Growth of Agrobacterium tumefaciens Is Determined by the 1,3-Diaminopropane Moiety. *ACS Chem Biol* **11**: 491-499.

Kuper, C. & K. Jung, (2005) CadC-mediated activation of the cadBA promoter in Escherichia coli. *J Mol Microbiol Biotechnol* **10**: 26-39.

Kwon, D.H. & C.D. Lu, (2006) Polyamines induce resistance to cationic peptide, aminoglycoside, and quinolone antibiotics in Pseudomonas aeruginosa PAO1. *Antimicrob Agents Chemother* **50**: 1615-1622.

Lee, J., A.J. Michael, D. Martynowski, E.J. Goldsmith & M.A. Phillips, (2007) Phylogenetic diversity and the structural basis of substrate specificity in the beta/alpha-barrel fold basic amino acid decarboxylases. *J Biol Chem* **282**: 27115-27125.

Lee, Y.S. & Y.D. Cho, (2001) Identification of essential active-site residues in ornithine decarboxylase of Nicotiana glutinosa decarboxylating both L-ornithine and L-lysine. *Biochem J* **360**: 657-665.

Letunic, I. & P. Bork, (2016) Interactive tree of life (iTOL) v3: an online tool for the display and annotation of phylogenetic and other trees. *Nucleic Acids Res* **44**: W242-245.

Liao, S., P. Poonpairoj, K.C. Ko, Y. Takatuska, Y. Yamaguchi, N. Abe, J. Kaneko & Y. Kamio, (2008) Occurrence of agmatine pathway for putrescine synthesis in Selenomonas ruminatium. *Biosci Biotechnol Biochem* **72**: 445-455.

Lightfoot, H.L. & J. Hall, (2014) Endogenous polyamine function--the RNA perspective. *Nucleic Acids Res* **42**: 11275-11290.

Lohinai, Z., B. Keremi, E. Szoko, T. Tabi, C. Szabo, Z. Tulassay, J.C. DiCesare, C.A. Davis, L.M. Collins & M. Levine, (2015) Biofilm Lysine Decarboxylase, a New Therapeutic Target for Periodontal Inflammation. *J Periodontol* **86**: 1176-1184.

Lu, C.D., Z. Yang & W. Li, (2004) Transcriptome analysis of the ArgR regulon in Pseudomonas aeruginosa. *J Bacteriol* **186**: 3855-3861.

Madhuri Indurthi, S., H.T. Chou & C.D. Lu, (2016) Molecular characterization of lysR-lysXE, gcdR-gcdHG and amaR-amaAB operons for lysine export and catabolism: a comprehensive lysine catabolic network in Pseudomonas aeruginosa PAO1. *Microbiology*

162: 876-888.
Malet, H., K. Liu, M. El Bakkouri, S.W. Chan, G. Effantin, M. Bacia, W.A. Houry & I. Gutsche, (2014) Assembly principles of a unique cage formed by hexameric and decameric E. coli proteins. *Elife* **3**: e03653.
Manuel, J., G.G. Zhanel & T. de Kievit, (2010) Cadaverine suppresses persistence to carboxypenicillins in Pseudomonas aeruginosa PAO1. *Antimicrob Agents Chemother* **54**: 5173-5179.
McClure MA, S.C., Elton P., (1996) Parameterization studies for the SAM and HMMER methods of hidden markov model generation. In: Proceedings / International Conference on Intelligent Systems for Molecular Biology. pp.
Merrell, D.S. & A. Camilli, (2000) Regulation of vibrio cholerae genes required for acid tolerance by a member of the "ToxR-like" family of transcriptional regulators. *J Bacteriol* **182**: 5342-5350.
Michael, A.J., (2016a) Biosynthesis of polyamines and polyamine-containing molecules. *Biochem J* **473**: 2315-2329.
Michael, A.J., (2016b) Polyamines in Eukaryotes, Bacteria, and Archaea. *J Biol Chem* **291**: 14896-14903.
Miller, J., (1972) Experiments in Molecular Genetics. In. C.S.H.L. Press (ed). Cold Spring Harbor, pp.
Nguyen, L.T., H.A. Schmidt, A. von Haeseler & B.Q. Minh, (2015) IQ-TREE: a fast and effective stochastic algorithm for estimating maximum-likelihood phylogenies. *Mol Biol Evol* **32**: 268-274.
Ochsner, U.A., M.L. Vasil, E. Alsabbagh, K. Parvatiyar & D.J. Hassett, (2000) Role of the Pseudomonas aeruginosa oxyR-recG operon in oxidative stress defense and DNA repair: OxyR-dependent regulation of katB-ankB, ahpB, and ahpC-ahpF. *J Bacteriol* **182**: 4533-4544.
Rahman, M. & P.H. Clarke, (1980) Genes and enzymes of lysine catabolism in Pseudomonas aeruginosa. *J Gen Microbiol* **116**: 357-369.
Ramulu, H.G., M. Groussin, E. Talla, R. Planel, V. Daubin & C. Brochier-Armanet, (2014) Ribosomal proteins: toward a next generation standard for prokaryotic systematics? *Mol Phylogenet Evol* **75**: 103-117.
Romano, A., V. Ladero, M.A. Alvarez & P.M. Lucas, (2014) Putrescine production via the ornithine decarboxylation pathway improves the acid stress survival of Lactobacillus brevis and is part of a horizontally transferred acid resistance locus. *Int J Food Microbiol* **175**: 14-19.
Romano, A., H. Trip, J.S. Lolkema & P.M. Lucas, (2013) Three-component lysine/ornithine decarboxylation system in Lactobacillus saerimneri 30a. *J Bacteriol* **195**: 1249-1254.
Ronquist, F. & J.P. Huelsenbeck, (2003) MrBayes 3: Bayesian phylogenetic inference under mixed models. *Bioinformatics* **19**: 1572-1574.
Schuster, M., A.C. Hawkins, C.S. Harwood & E.P. Greenberg, (2004) The Pseudomonas aeruginosa RpoS regulon and its relationship to quorum sensing. *Mol Microbiol* **51**: 973-985.
Sekowska, A., P. Bertin & A. Danchin, (1998) Characterization of polyamine synthesis pathway in Bacillus subtilis 168. *Mol Microbiol* **29**: 851-858.
Seo, H. & K.J. Kim, (2017) Structural basis for a novel type of cytokinin-activating protein. *Sci Rep* **7**: 45985.
Sevin, D.C., T. Fuhrer, N. Zamboni & U. Sauer, (2017) Nontargeted in vitro metabolomics for

high-throughput identification of novel enzymes in Escherichia coli. *Nat Methods* **14**: 187-194.

Shah, P. & E. Swiatlo, (2008) A multifaceted role for polyamines in bacterial pathogens. *Mol Microbiol* **68**: 4-16.

Shan, Y., A. Brown Gandt, S.E. Rowe, J.P. Deisinger, B.P. Conlon & K. Lewis, (2017) ATP-Dependent Persister Formation in Escherichia coli. *MBio* **8**.

Snider, J., I. Gutsche, M. Lin, S. Baby, B. Cox, G. Butland, J. Greenblatt, A. Emili & W.A. Houry, (2006) Formation of a distinctive complex between the inducible bacterial lysine decarboxylase and a novel AAA+ ATPase. *J Biol Chem* **281**: 1532-1546.

Soksawatmaekhin, W., A. Kuraishi, K. Sakata, K. Kashiwagi & K. Igarashi, (2004) Excretion and uptake of cadaverine by CadB and its physiological functions in Escherichia coli. *Mol Microbiol* **51**: 1401-1412.

Stover, C.K., X.Q. Pham, A.L. Erwin, S.D. Mizoguchi, P. Warrener, M.J. Hickey, F.S. Brinkman, W.O. Hufnagle, D.J. Kowalik, M. Lagrou, R.L. Garber, L. Goltry, E. Tolentino, S. Westbrock-Wadman, Y. Yuan, L.L. Brody, S.N. Coulter, K.R. Folger, A. Kas, K. Larbig, R. Lim, K. Smith, D. Spencer, G.K. Wong, Z. Wu, I.T. Paulsen, J. Reizer, M.H. Saier, R.E. Hancock, S. Lory & M.V. Olson, (2000) Complete genome sequence of Pseudomonas aeruginosa PAO1, an opportunistic pathogen. *Nature* **406**: 959-964.

Sugawara, A., D. Matsui, N. Takahashi, M. Yamada, Y. Asano & K. Isobe, (2014) Characterization of a pyridoxal-5'-phosphate-dependent l-lysine decarboxylase/oxidase from Burkholderia sp. AIU 395. *J Biosci Bioeng* **118**: 496-501.

Tabor, C.W. & H. Tabor, (1985) Polyamines in microorganisms. *Microbiol Rev* **49**: 81-99.

Tabor, H., E.W. Hafner & C.W. Tabor, (1980) Construction of an Escherichia coli strain unable to synthesize putrescine, spermidine, or cadaverine: characterization of two genes controlling lysine decarboxylase. *J Bacteriol* **144**: 952-956.

Tabor, H. & C.W. Tabor, (1964) Spermidine, Spermine, and Related Amines. *Pharmacol Rev* **16**: 245-300.

Takatsuka, Y., Y. Yamaguchi, M. Ono & Y. Kamio, (2000) Gene cloning and molecular characterization of lysine decarboxylase from Selenomonas ruminantium delineate its evolutionary relationship to ornithine decarboxylases from eukaryotes. *J Bacteriol* **182**: 6732-6741.

Thibault, J., E. Faudry, C. Ebel, I. Attree & S. Elsen, (2009) Anti-activator ExsD forms a 1:1 complex with ExsA to inhibit transcription of type III secretion operons. *J Biol Chem* **284**: 15762-15770.

Valot, B., C. Guyeux, J.Y. Rolland, K. Mazouzi, X. Bertrand & D. Hocquet, (2015) What It Takes to Be a Pseudomonas aeruginosa? The Core Genome of the Opportunistic Pathogen Updated. *PLoS One* **10**: e0126468.

Viala, J.P., S. Meresse, B. Pocachard, A.A. Guilhon, L. Aussel & F. Barras, (2011) Sensing and adaptation to low pH mediated by inducible amino acid decarboxylases in Salmonella. *PLoS One* **6**: e22397.

Zhao, B. & W.A. Houry, (2010) Acid stress response in enteropathogenic gammaproteobacteria: an aptitude for survival. *Biochem Cell Biol* **88**: 301-314.

Acknowledgments: we thank Rémi Peyraud and Ina Attrée for helpful discussions. This work has received funding from GRAL (ANR-10-LABX-49-01), the European Union's Horizon 2020 research and innovation programme under grant agreement No 647784, and the ANR-16-CE02-0005. This work was also supported by CEA and the French Ministry of Research and National Research Agency as part of the French metabolomics and fluxomics infrastructure (MetaboHUB, ANR-11-INBS-0010 grant). Diego Carriel was supported by a PhD grant from LABEX GRAL and Pierre S. Garcia was supported by a PhD grant from ARC1 Santé Rhône-Alpes Auvergne.

Author contributions: DCL, PSG, FC, and PL performed experiments. All authors analyzed data. IG, SE and CBA designed and supervised the overall study and wrote the paper with contribution from all authors.

Abbreviated Summary

Bacterial polyamines are involved in many fundamental processes and are mainly synthetized by dedicated lysine, arginine and ornithine decarboxylases or LAOdcs. Our exhaustive phylogenetic analysis reveals evolutionary history of LAOdcs and discloses a hitherto overlooked LdcA subfamily. We show that LdcA is playing an important role in growth and persistence of the major multidrug resistant human pathogen *P. aeruginosa*, exerted through cadaverine biosynthesis and concomitant regulation of intracellular levels of putrescine and spermidine.

Figure legends

Fig. 1. LAOdc is a widespread family in Bacteria

A. Taxonomic distribution in Prokaryotes. Ratio corresponds to the number of proteomes containing at least one homologue on the number of proteomes present in our database for each phylum. Phyla represented by at least 10 proteomes, among which more than 20% contained at least one LAOdc homologue are highlighted by colors.

B. Unrooted ML tree of LAOdcs (PhyML, LG+I+G4 according to BIC, 1,117 sequences, 273 amino-acid positions). The tree can be divided in three parts: Cluster I corresponds to wing-less LAOdc mainly from *Firmicutes*, *Actinobacteria* and *Cyanobacteria*; Cluster II encompasses wing domain containing LAOdc mainly from *Proteobacteria*, while Cluster III gathers wing-less and wing domain-containing LAOdc from various and unrelated taxa. The scale bar represents the number of substitutions per site. Numbers at branches correspond to bootstrap values (BV).

Fig. 2. Phylogeny of proteobacterial LAOdc (Cluster II)

A. ML phylogeny of cluster II LAOdc (PhyML, LG+I+G4 according to BIC, 551 sequences, 589 amino-acid positions). LAOdc sequences from *E. coli* and *P. aeruginosa* are indicated with gray arrows. Red circles represent bootstrap values.

B. Bayesian phylogeny of Cluster II LAOdc sequences inferred from a sample of representative species. The tree is rooted with LAOdc sequences from Cluster I and III (see also Fig. 1) (MrBayes, mixed model+G4, 54 sequences, 392 amino acid positions). The scale bar represents the number of substitutions per site. Numbers at branches represent posterior probabilities values.

915

916 **Fig. 3.** Evolutionary scenario of LAOdcs in *Proteobacteria*

917 A. Phylogeny in *Proteobacteria* based on ribosomal proteins (PhyML, LG+I+G4 according to BIC,
918 108 sequences, 6,129 amino acid positions). Green: *Deltaproteobacteria*, light green:
919 *Epsilonproteobacteria*, violet: *Alphaproteobacteria*, red: *Betaproteobacteria*, blue:
920 *Gammaproteobacteria*. Red circles: BV (Bootstrap value), blue diamond: ancestral presence,
921 rectangle: at least one genome possessing at least one copy of LAOdc, green rectangle:
922 ancestral presence, red rectangle: secondary acquisition by horizontal gene transfer. Leaves
923 correspond to families.

924 B. Evolutive scenario of LAOdc in Enterobacteraceae (PhyML, LG+I+G4 according to BIC, 34
925 sequences, 6333 amino acid positions). Leaves correspond to genius. Red circles: BV (Bootstrap
926 value), blue diamond: ancestral acquisition, rectangle: at least one genome possessing at least
927 one copy of LAOdc, green rectangle: ancestral presence, red rectangle: secondary acquisition by
928 horizontal gene transfer.

929

930 **Fig. 4.** Genomic context of LAOdc genes from Cluster II

931 Colored arrows correspond to conserved neighbor genes. Black arrows correspond to LAOdc
932 considered gene.

933

934 **Fig. 5.** Factors influencing *ldcA* expression

935 Activity of *ldcA* promoter fused to *lacZ* reporter gene was assessed during growth in different
936 media and genetic backgrounds. Measurements of the β-galactosidase activity of PAO1*::PldcA-*

937 *lacZ* strain grown either in minimal medium P (MMP) containing 20 mM L-glutamate and 20 mM
938 arginine (A), or in LB containing or not 20 mM arginine (B) were performed at times indicated.
939 C. β-galactosidase activity of wild-type and indicated mutant CHA strains harboring the *PldcA-*
940 *lacZ* fusion and grown in LB. β-galactosidase activity is expressed in Miller Units (left Y-axis) and
941 presented in the bar graphs. Growth was performed in 125 ml flasks, followed by measure of
942 OD_{600} (right Y-axis) and plotted on lines. Results are the average of values from three
943 independent experiments ± standard deviation (SD).
944
945 **Fig. 6.** Intracellular Cad in rich medium is produced by the lysine decarboxylase LdcA
946 A. Growth curves of the wild-type strain, the *ldcA* mutant and the complemented strain in the
947 rich Mueller Hinton medium.
948 B. Intracellular concentration, expressed in area of chromatogram peak, of the three indicated
949 polyamines at (1) early-, (2) mid- and (3) late-exponential growth phases as indicated.
950
951 **Fig. 7.** Polyamines are important for growth fitness in minimal medium
952 Growth of the wild-type PAO1 strain, the *ldcA* mutant and the complemented strain in minimal
953 MMP medium supplemented with 20 mM glutamate, 1mM arginine and 5 mM of (A) lysine, (B)
954 Cad, (C) Put or (D) Spd in 96-well plates. The experiments are representative of two
955 experiments.
956
957
958 **Supporting informations**

959 **Supplemental material and methods**

960

961 **FIG S1.** LAOdcs are ancestral in *Cyanobacteria*. (A) Taxonomic distribution of LAOdc in
962 *Cyanobacteria* (PhyML, LG+I+G4 according to BIC, 30 sequences, 6394 amino acid positions).
963 Leaves correspond to genera. Red circles: BV (Bootstrap value), blue diamond: ancestral
964 acquisition, rectangle: at least one genome possessing at least one copy of LAOdc, green
965 rectangle: ancestral presence. (B) Phylogeny of LAOdc of *Cyanobacteria* (PhyML, LG+I+G4
966 according to BIC, 28 sequences, 446 amino-acid positions). (C) Genomic context of LAOdc in
967 three *Cyanobacteria*. Black arrows: LAOdc gene.

968

969 **FIG S2.** LAOdcs are ancestral in *Firmicutes*. (A) Taxonomic distribution of LAOdc in *Firmicutes*
970 (PhyML, LG+I+G4 according to BIC, 38 sequences, 6133 amino-acid positions). Brown:
971 *Natranaerobiales* and *Halanaerobiales*, green and blue: *Clostridia*, red: *Bacillales*, pink:
972 *Lactobacillales*. Red circles: BV (Bootstrap value), blue diamond: ancestral acquisition, rectangle:
973 at least one genome possessing at least one copy of LAOdc, green rectangle: ancestral presence,
974 red rectangle: horizontal acquisition. (B) Phylogeny of LAOdc Cluster I (PhyML, LG+I+G4
975 according to BIC, 504 sequences, 295 amino-acid positions). Leaves color correspond to species
976 families. Gray leaves represent non-*Firmicutes* sequences. Ring color correspond to paralogue A
977 (blue) and B (red). (C) Genomic context of LAOdc A and B in *Firmicutes*. Black arrows: LAOdc
978 gene, colored arrows: conserved neighbor genes.

979

980 **FIG S3** Evolutionary origin of *Firmicutes* OdcI sequences from *Proteobacteria*. (PhyML, LG+I+G4

981 according to BIC, 514 sequences, 583 amino-acid positions). Blue leaves: *Proteobacteria*, red
982 leaves: *Firmicutes*. Gray arrows indicate the position of the two copies of LAOdc of *Lactobacillus*
983 *saerimneri*. Pink: OdcC, green: LdcA, red: Adc, blue: OdcI/C. The scale bar indicates the number
984 of substitutions per site. Numbers at branches correspond to aLRT supports.
985
986 **FIG S4** Influence of stress on *ldcA* expression and growth fitness of *P. aeruginosa*. (A) Effect of
987 acid and oxidative stress during growth in rich medium. At T_0, HCl was added to shift the pH of
988 LB medium from neutral to pH 5 while H_2O_2 was added to a final entration of 1mM. β-
989 galactosidase activity of PAO1*::PldcA-lacZ* strain was measured at T_0, then monitored 30 and 60
990 min after treatment. B) Growth of PAO1 in minimal medium at different pHs was evaluated
991 using Biolog high-throughput system. Each point corresponds to the "Area Under the Curve"
992 (AUC) measured after 24h of bacterial growth.
993
994 **FIG S5** LdcA function affects carbenicillin persistence. Percentage of survivors in rich medium
995 (cation-adjusted Mueller Hinton Broth) after 24h of carbenicillin treatment. Growth was
996 performed in erlenmeyer flasks at 37°C with agitation (300 RPM). Percentage of survivors was
997 calculated from CFU counting after 24h of antibiotic treatment at 500µg/ml (8X MIC).
998
999 **Table S1** AAT-fold LAOdc homologues in prokaryotes.
1000 **Table S2** List of bacterial strains and plasmids used in this work.
1001 **Table S3** Primers used in this study.
1002

A

Phylum	ratio
Proteobacteria	323/778
Alphaproteobacteria	30/205
Betaproteobacteria	120/135
Gammaproteobacteria	172/342
Deltaproteobacteria	1/56
Epsilonproteobacteria	0/38

Phylum	ratio
Firmicutes	233/307
Cyanobacteria	39/39
Actinobacteria	62/230
Other bacteria	26/366
Archaea	0/166

B

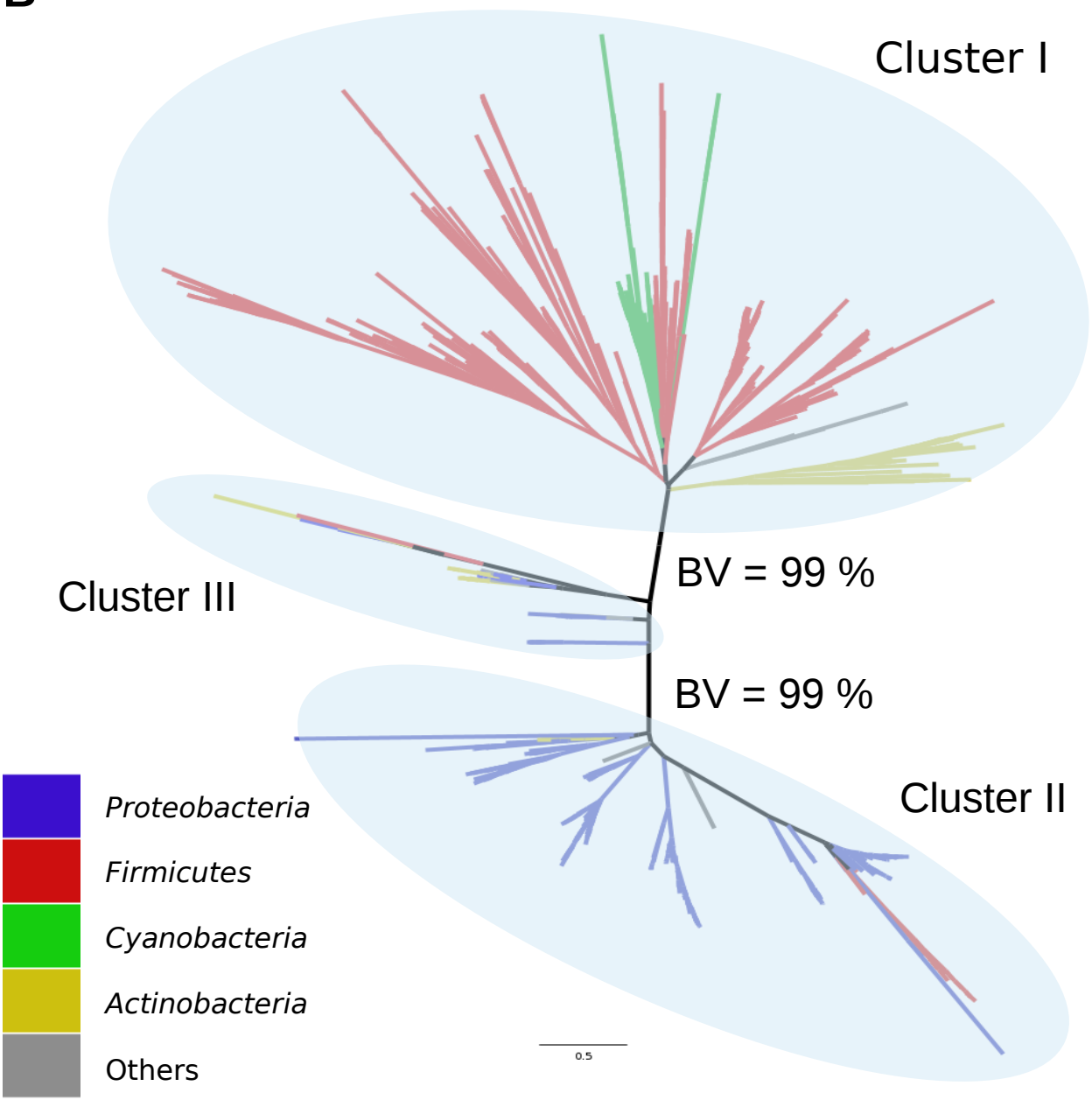

A

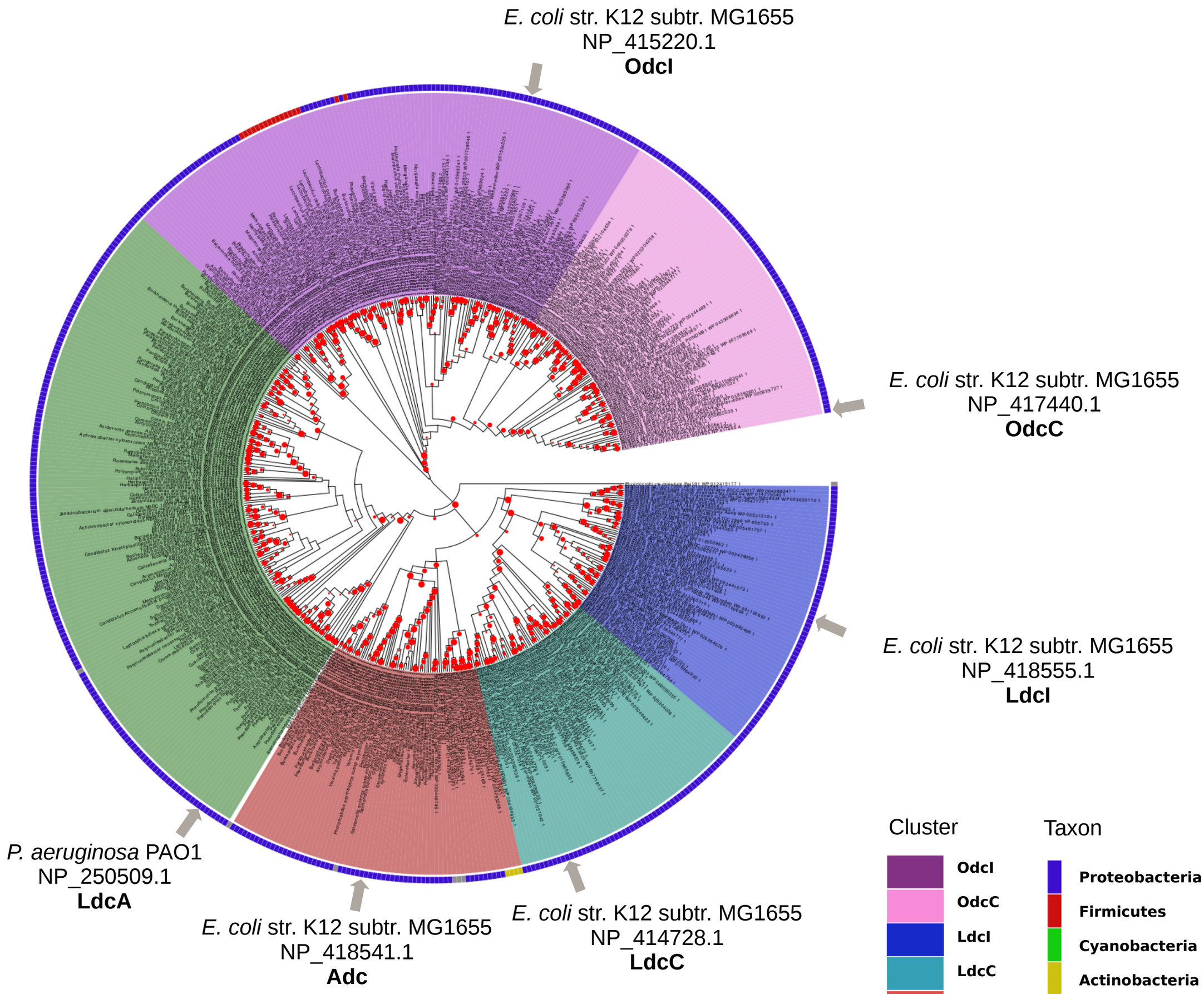
E. coli str. K12 subtr. MG1655
NP_415220.1
OdcI
E. coli str. K12 subtr. MG1655
NP_417440.1
OdcC
E. coli str. K12 subtr. MG1655
NP_418555.1
LdcI
P. aeruginosa PAO1
NP_250509.1
LdcA
E. coli str. K12 subtr. MG1655
NP_418541.1
Adc
E. coli str. K12 subtr. MG1655
NP_414728.1
LdcC
Cluster
OdcI
OdcC
LdcI
LdcC
Adc
LdcA
Taxon
Proteobacteria
Firmicutes
Cyanobacteria
Actinobacteria
Others

B

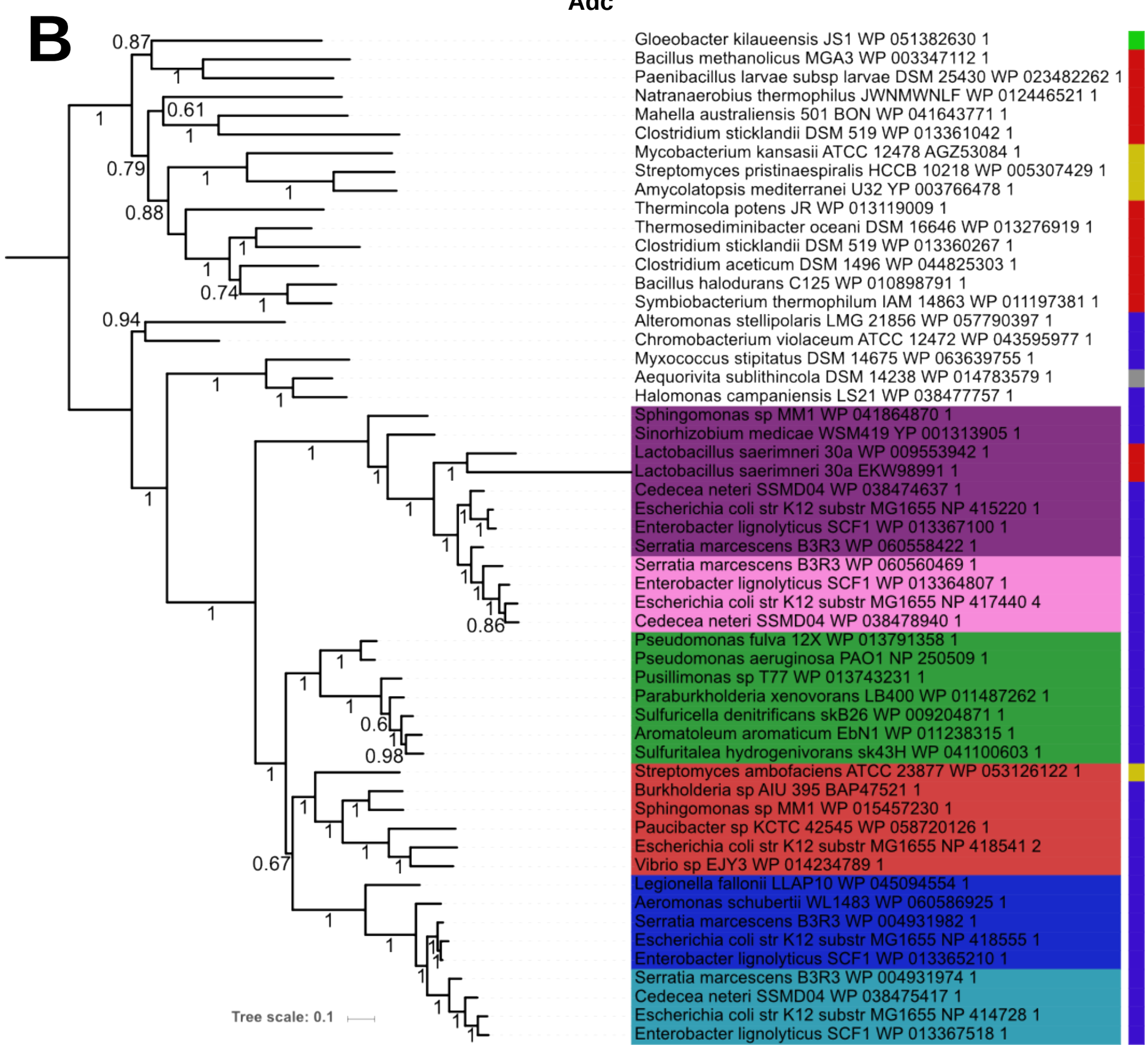
Gloeobacter kilaueensis JS1 WP 051382630 1
Bacillus methanolicus MGA3 WP 003347112 1
Paenibacillus larvae subsp larvae DSM 25430 WP 023482262 1
Natranaerobius thermophilus JWNMWNLF WP 012446521 1
Mahella australiensis 501 BON WP 041643771 1
Clostridium sticklandii DSM 519 WP 013361042 1
Mycobacterium kansasii ATCC 12478 AGZ53084 1
Streptomyces pristinaespiralis HCCB 10218 WP 005307429 1
Amycolatopsis mediterranei U32 YP 003766478 1
Thermincola potens JR WP 013119009 1
Thermosediminibacter oceani DSM 16646 WP 013276919 1
Clostridium sticklandii DSM 519 WP 013360267 1
Clostridium aceticum DSM 1496 WP 044825303 1
Bacillus halodurans C125 WP 010898791 1
Symbiobacterium thermophilum IAM 14863 WP 011197381 1
Alteromonas stellipolaris LMG 21856 WP 057790397 1
Chromobacterium violaceum ATCC 12472 WP 043595977 1
Myxococcus stipitatus DSM 14675 WP 063639755 1
Aequorivita sublithincola DSM 14238 WP 014783579 1
Halomonas campaniensis LS21 WP 038477757 1
Sphingomonas sp MM1 WP 041864870 1
Sinorhizobium medicae WSM419 YP 001313905 1
Lactobacillus saerimneri 30a WP 009553942 1
Lactobacillus saerimneri 30a EKW98991 1
Cedecea neteri SSMD04 WP 038474637 1
Escherichia coli str K12 substr MG1655 NP 415220 1
Enterobacter lignolyticus SCF1 WP 013367100 1
Serratia marcescens B3R3 WP 060558422 1
Serratia marcescens B3R3 WP 060560469 1
Enterobacter lignolyticus SCF1 WP 013364807 1
Escherichia coli str K12 substr MG1655 NP 417440 4
Cedecea neteri SSMD04 WP 038478940 1
Pseudomonas fulva 12X WP 013791358 1
Pseudomonas aeruginosa PAO1 NP 250509 1
Pusillimonas sp T77 WP 013743231 1
Paraburkholderia xenovorans LB400 WP 011487262 1
Sulfuricella denitrificans skB26 WP 009204871 1
Aromatoleum aromaticum EbN1 WP 011238315 1
Sulfuritalea hydrogenivorans sk43H WP 041100603 1
Streptomyces ambofaciens ATCC 23877 WP 053126122 1
Burkholderia sp AIU 395 BAP47521 1
Sphingomonas sp MM1 WP 015457230 1
Paucibacter sp KCTC 42545 WP 058720126 1
Escherichia coli str K12 substr MG1655 NP 418541 2
Vibrio sp EJY3 WP 014234789 1
Legionella fallonii LLAP10 WP 045094554 1
Aeromonas schubertii WL1483 WP 060586925 1
Serratia marcescens B3R3 WP 004931982 1
Escherichia coli str K12 substr MG1655 NP 418555 1
Enterobacter lignolyticus SCF1 WP 013365210 1
Serratia marcescens B3R3 WP 004931974 1
Cedecea neteri SSMD04 WP 038475417 1
Escherichia coli str K12 substr MG1655 NP 414728 1
Enterobacter lignolyticus SCF1 WP 013367518 1
Tree scale: 0.1

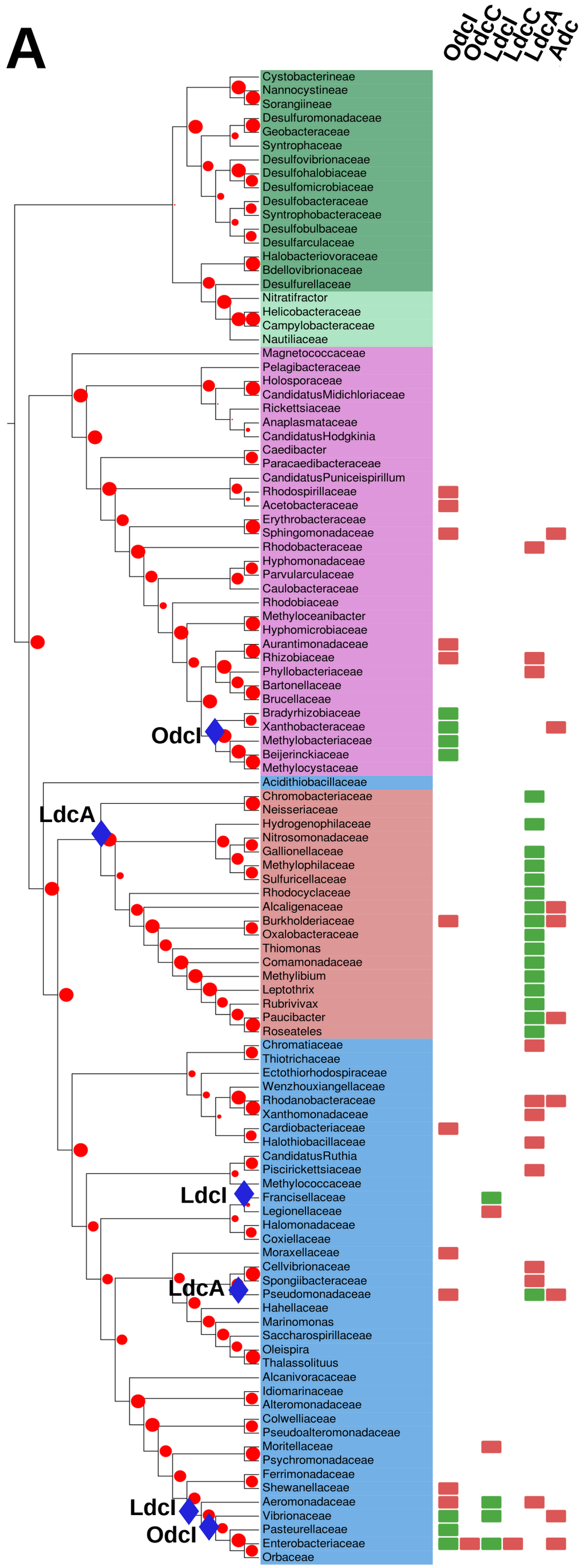
A
OdcI
OdcC
LdcI
LdcC
LdcA
Adc
Cystobacterineae
Nannocystineae
Sorangiineae
Desulfuromonadaceae
Geobacteraceae
Syntrophaceae
Desulfovibrionaceae
Desulfohalobiaceae
Desulfomicrobiaceae
Desulfobacteraceae
Syntrophobacteraceae
Desulfobulbaceae
Desulfarculaceae
Halobacteriovoraceae
Bdellovibrionaceae
Desulfurellaceae
Nitratifractor
Helicobacteraceae
Campylobacteraceae
Nautiliaceae
Magnetococcaceae
Pelagibacteraceae
Holosporaceae
CandidatusMidichloriaceae
Rickettsiaceae
Anaplasmataceae
CandidatusHodgkinia
Caedibacter
Paracaedibacteraceae
CandidatusPuniceispirillum
Rhodospirillaceae
Acetobacteraceae
Erythrobacteraceae
Sphingomonadaceae
Rhodobacteraceae
Hyphomonadaceae
Parvularculaceae
Caulobacteraceae
Rhodobiaceae
Methyloceanibacter
Hyphomicrobiaceae
Aurantimonadaceae
Rhizobiaceae
Phyllobacteriaceae
Bartonellaceae
Brucellaceae
Bradyrhizobiaceae
Xanthobacteraceae
Methylobacteriaceae
Beijerinckiaceae
Methylocystaceae
OdcI
Acidithiobacillaceae
Chromobacteriaceae
Neisseriaceae
Hydrogenophilaceae
Nitrosomonadaceae
Gallionellaceae
Methylophilaceae
Sulfuricellaceae
Rhodocyclaceae
Alcaligenaceae
Burkholderiaceae
Oxalobacteraceae
Thiomonas
Comamonadaceae
Methylibium
Leptothrix
Rubrivivax
Paucibacter
Roseateles
LdcA
Chromatiaceae
Thiotrichaceae
Ectothiorhodospiraceae
Wenzhouxiangellaceae
Rhodanobacteraceae
Xanthomonadaceae
Cardiobacteriaceae
Halothiobacillaceae
CandidatusRuthia
Piscirickettsiaceae
Methylococcaceae
Francisellaceae
Legionellaceae
Halomonadaceae
Coxiellaceae
LdcI
Moraxellaceae
Cellvibrionaceae
Spongiibacteraceae
Pseudomonadaceae
LdcA
Hahellaceae
Marinomonas
Saccharospirillaceae
Oleispira
Thalassolituus
Alcanivoracaceae
Idiomarinaceae
Alteromonadaceae
Colwelliaceae
Pseudoalteromonadaceae
Moritellaceae
Psychromonadaceae
Ferrimonadaceae
Shewanellaceae
Aeromonadaceae
Vibrionaceae
Pasteurellaceae
Enterobacteriaceae
Orbaceae
LdcI
OdcI

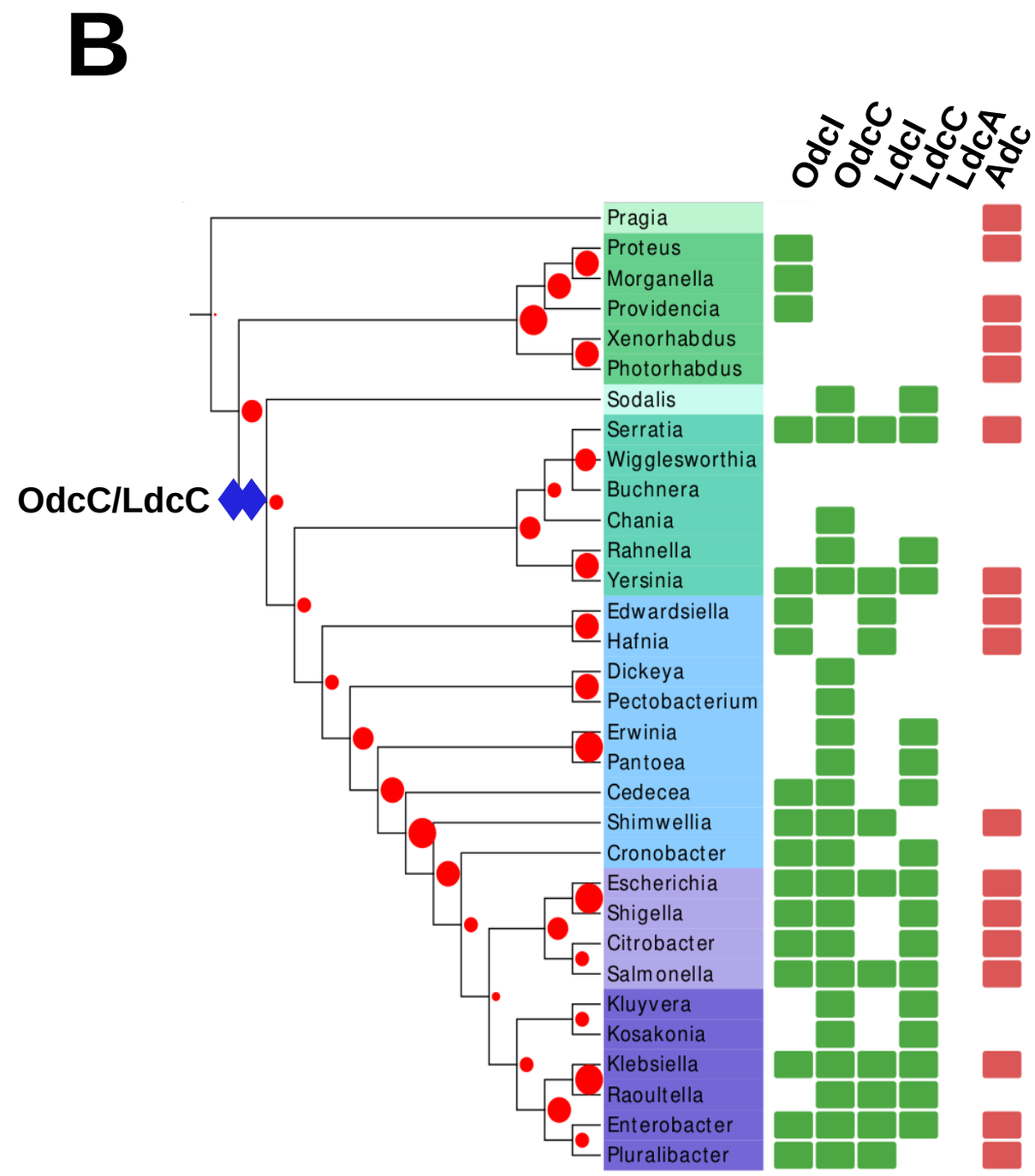
B
OdcI
OdcC
LdcI
LdcC
LdcA
Adc
Pragia
Proteus
Morganella
Providencia
Xenorhabdus
Photorhabdus
Sodalis
Serratia
Wigglesworthia
Buchnera
Chania
Rahnella
Yersinia
Edwardsiella
Hafnia
Dickeya
Pectobacterium
Erwinia
Pantoea
Cedecea
Shimwellia
Cronobacter
Escherichia
Shigella
Citrobacter
Salmonella
Kluyvera
Kosakonia
Klebsiella
Raoultella
Enterobacter
Pluralibacter
OdcC/LdcC

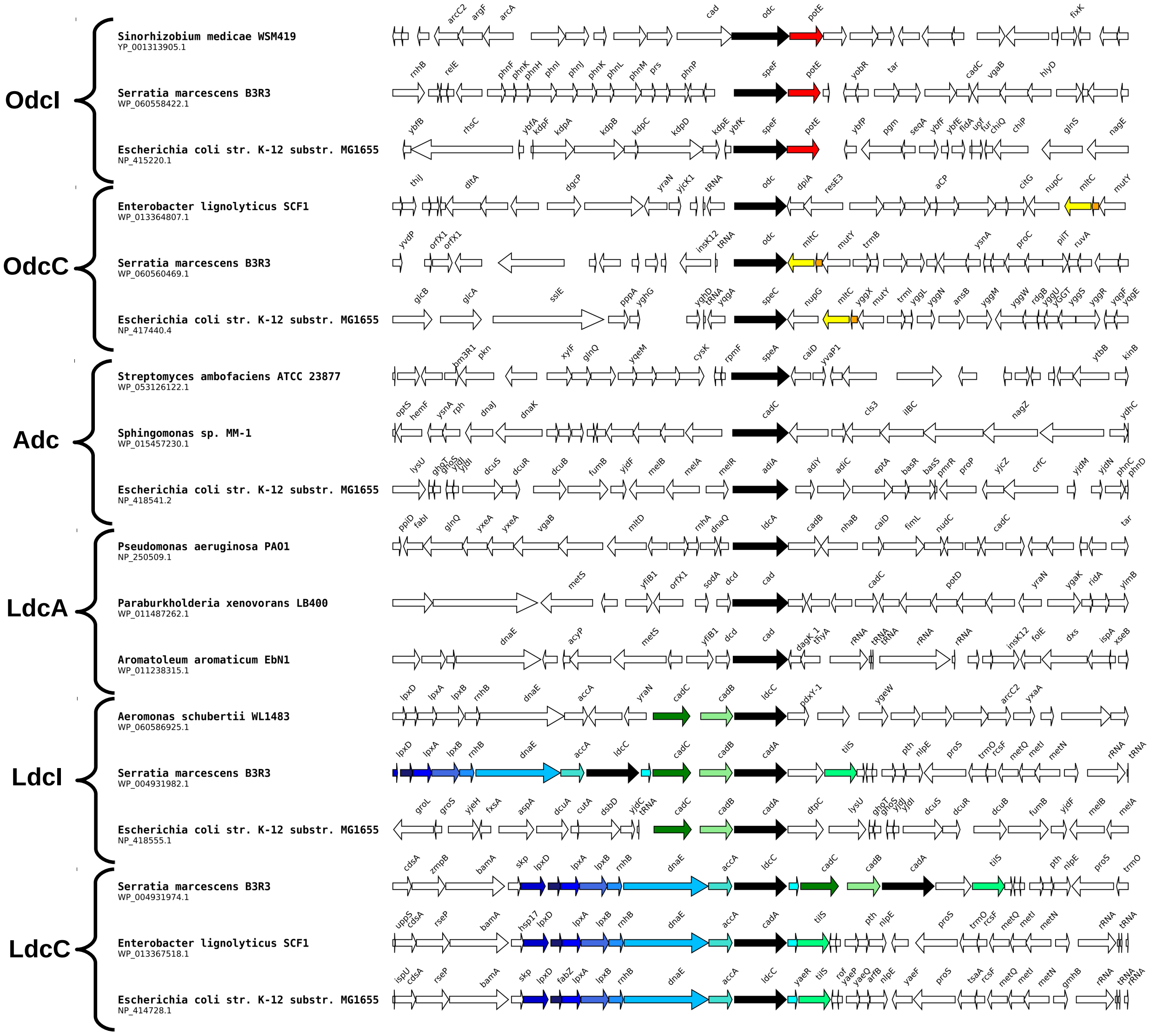
OdcI
Sinorhizobium medicae WSM419
YP_001313905.1
arcC2 argF arcA cad odc potE fixK
Serratia marcescens B3R3
WP_060558422.1
rnhB relE phnF phnK phnH phnI phnJ phnK phnL phnM prs phnP speF potE yobR tar cadC vgaB hlyD
Escherichia coli str. K-12 substr. MG1655
NP_415220.1
ybfB rhsC ybfA kdpF kdpA kdpB kdpC kdpD kdpE ybfK speF potE ybfP pgm seqA ybfF ybfE fldA ugf fur chiQ chiP glnS nagE
OdcC
Enterobacter lignolyticus SCF1
WP_013364807.1
thiJ dltA dgcP yraN yjcK1 tRNA odc dpiA resE3 aCP citG nupC mltC mutY
Serratia marcescens B3R3
WP_060560469.1
yvdP orfX1 orfX1 insK12 tRNA odc mltC mutY trmB ysnA proC pilT ruvA
Escherichia coli str. K-12 substr. MG1655
NP_417440.4
glcB glcA sslE pppA yghG yghD tRNA yqgA speC nupG mltC yggX mutY trmI yggL yggN ansB yggM yggW rdgB yggU YGGT yggS yggR yqgF yqgE
Adc
Streptomyces ambofaciens ATCC 23877
WP_053126122.1
bm3R1 pkn xylF glnQ yqeM cysK rpmF speA caiD yvaP1 ytbB kinB
Sphingomonas sp. MM-1
WP_015457230.1
optS hemF ysnA rph dnaJ dnaK cadC cls3 ilBC nagZ ydhC
Escherichia coli str. K-12 substr. MG1655
NP_418541.2
lysU ghoT ghoS yjdI yjdI dcuS dcuR dcuB fumB yjdF melB melA melR adiA adiY adiC eptA basR basS pmrR proP yicZ crfC yjdM yjdN phnC phnD
LdcA
Pseudomonas aeruginosa PAO1
NP_250509.1
ppiD fabI glnQ yxeA yxeA vgaB mltD rnhA dnaQ ldcA cadB nhaB caiD fimL nudC cadC tar
Paraburkholderia xenovorans LB400
WP_011487262.1
metS yfiB1 orfX1 sodA dcd cad cadC potD yraN ygaK ridA ylmB
Aromatoleum aromaticum EbN1
WP_011238315.1
dnaE acyP metS yfiB1 dcd cad dagK_1 thyA rRNA tRNA tRNA rRNA rRNA insK12 folE dxs ispA xseB
LdcI
Aeromonas schubertii WL1483
WP_060586925.1
lpxD lpxA lpxB rnhB dnaE accA yraN cadC cadB ldcC pdxY-1 ygeW arcC2 yxaA
Serratia marcescens B3R3
WP_004931982.1
lpxD lpxA lpxB rnhB dnaE accA ldcC cadC cadB cadA tilS pth nlpE proS trmO rcsF metQ metI metN rRNA tRNA
Escherichia coli str. K-12 substr. MG1655
NP_418555.1
groL groS yjeH fxsA aspA dcuA cutA dsbD yjdC tRNA cadC cadB cadA dtpC lysU ghoT ghoS yjdI yjdI dcuS dcuR dcuB fumB yjdF melB melA
LdcC
Serratia marcescens B3R3
WP_004931974.1
cdsA zmpB bamA skp lpxD lpxA lpxB rnhB dnaE accA ldcC cadC cadB cadA tilS pth nlpE proS trmO
Enterobacter lignolyticus SCF1
WP_013367518.1
uppS cdsA rseP bamA hsp17 lpxD lpxA lpxB rnhB dnaE accA cadA tilS pth nlpE proS trmO rcsF metQ metI metN rRNA tRNA
Escherichia coli str. K-12 substr. MG1655
NP_414728.1
ispU cdsA rseP bamA skp lpxD fabZ lpxA lpxB rnhB dnaE accA ldcC yaeR tilS rof yaeP yaeQ arfB nlpE yaeF proS tsaA rcsF metQ metI metN gmhB rRNA tRNA rRNA

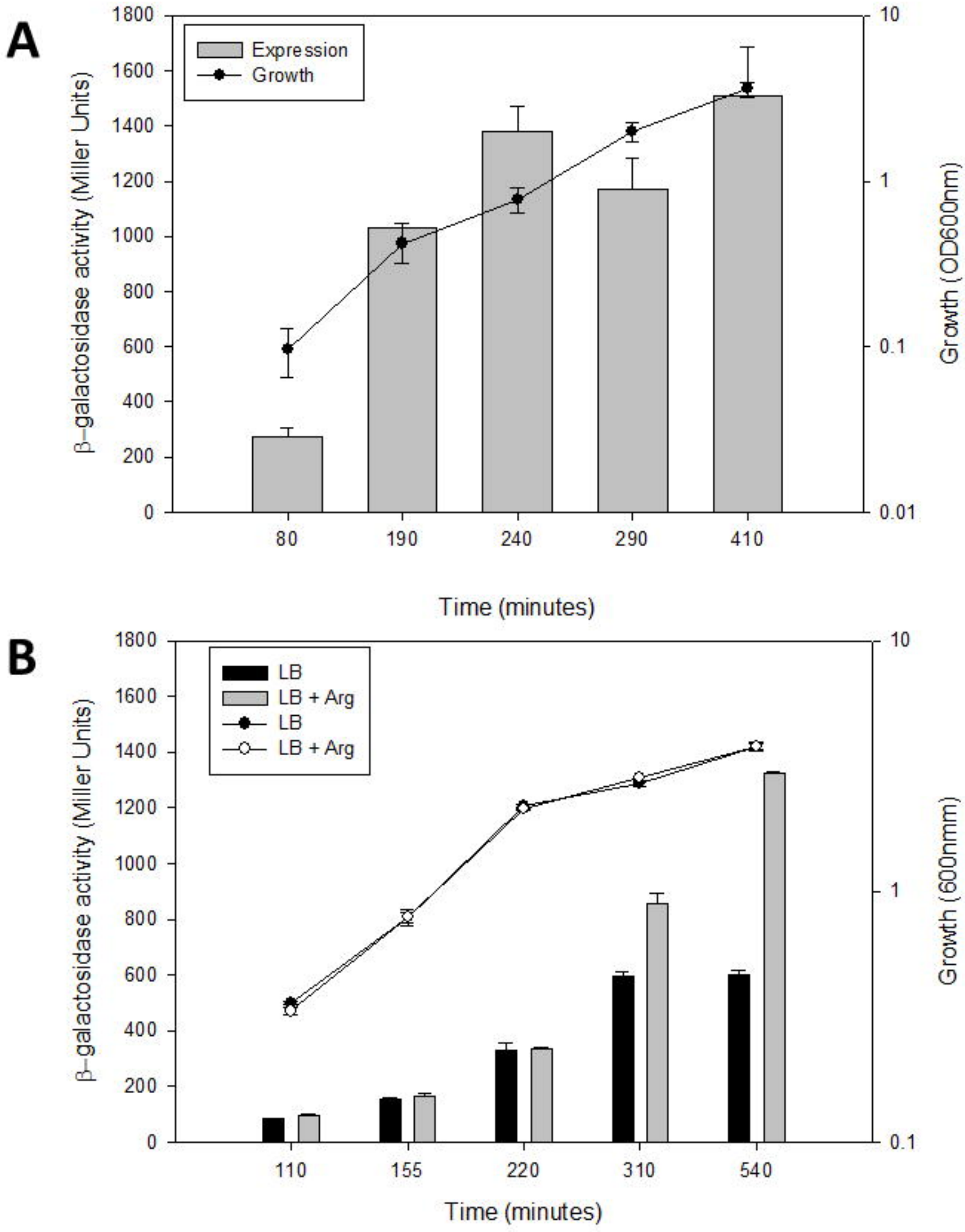
A
Expression
Growth
β–galactosidase activity (Miller Units)
Growth (OD600nm)
Time (minutes)
80
190
240
290
410
B
LB
LB + Arg
LB
LB + Arg
β–galactosidase activity (Miller Units)
Growth (600nmm)
Time (minutes)
110
155
220
310
540

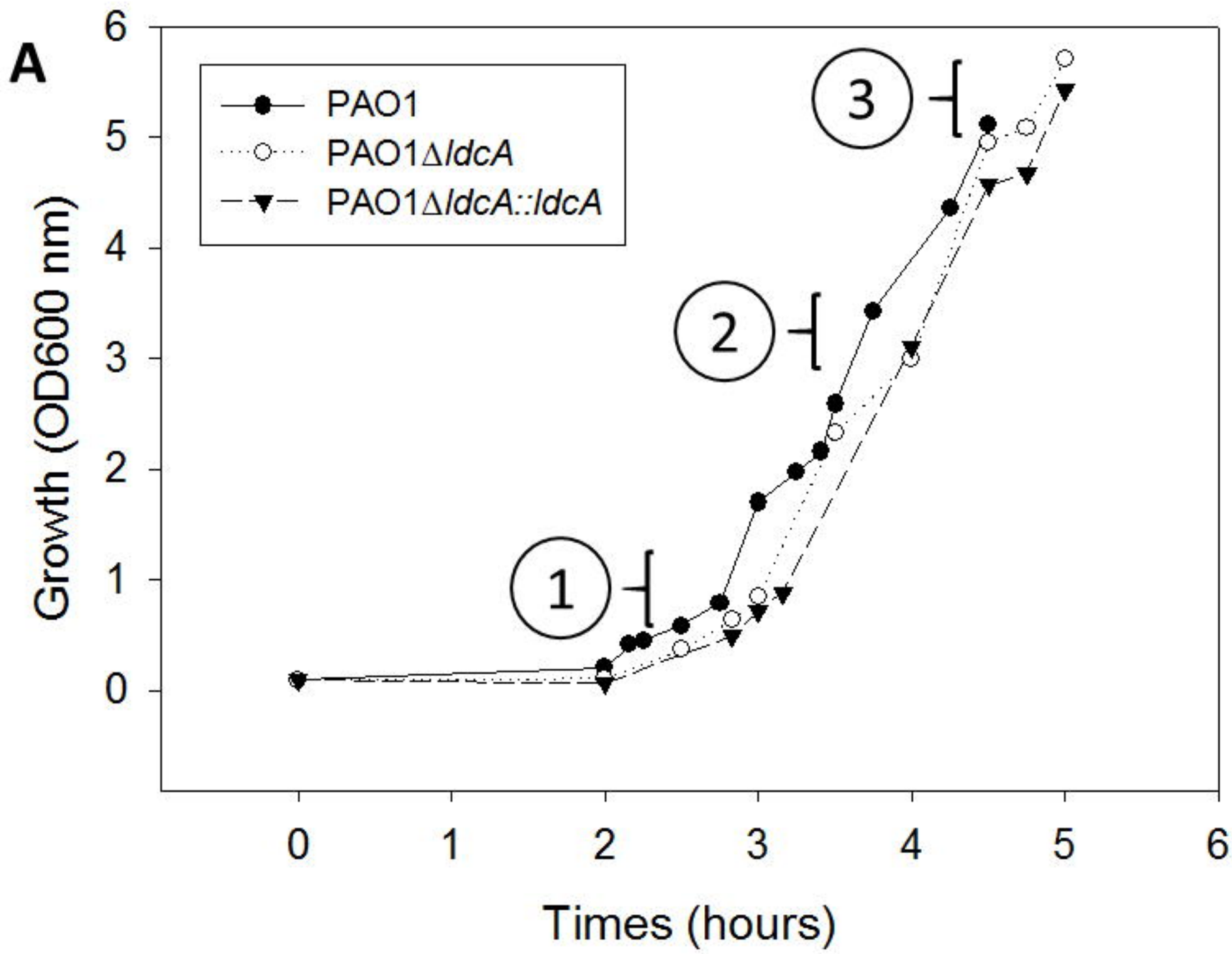
A
PAO1
PAO1ΔldcA
PAO1ΔldcA::ldcA
Growth (OD600 nm)
Times (hours)
3
2
1

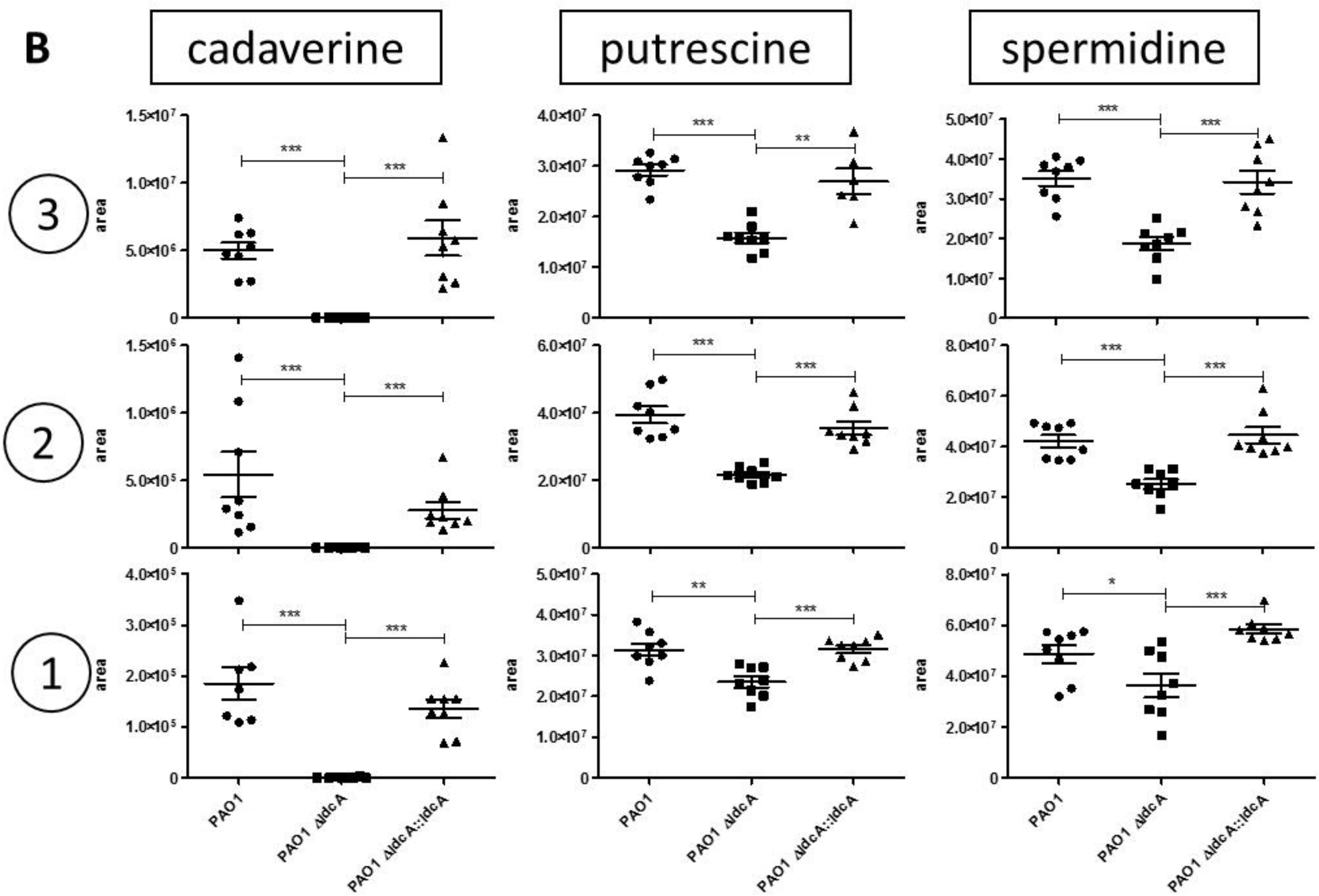
B
cadaverine
putrescine
spermidine
3
2
1
area
PAO1
PAO1 ΔldcA
PAO1 ΔldcA::ldcA

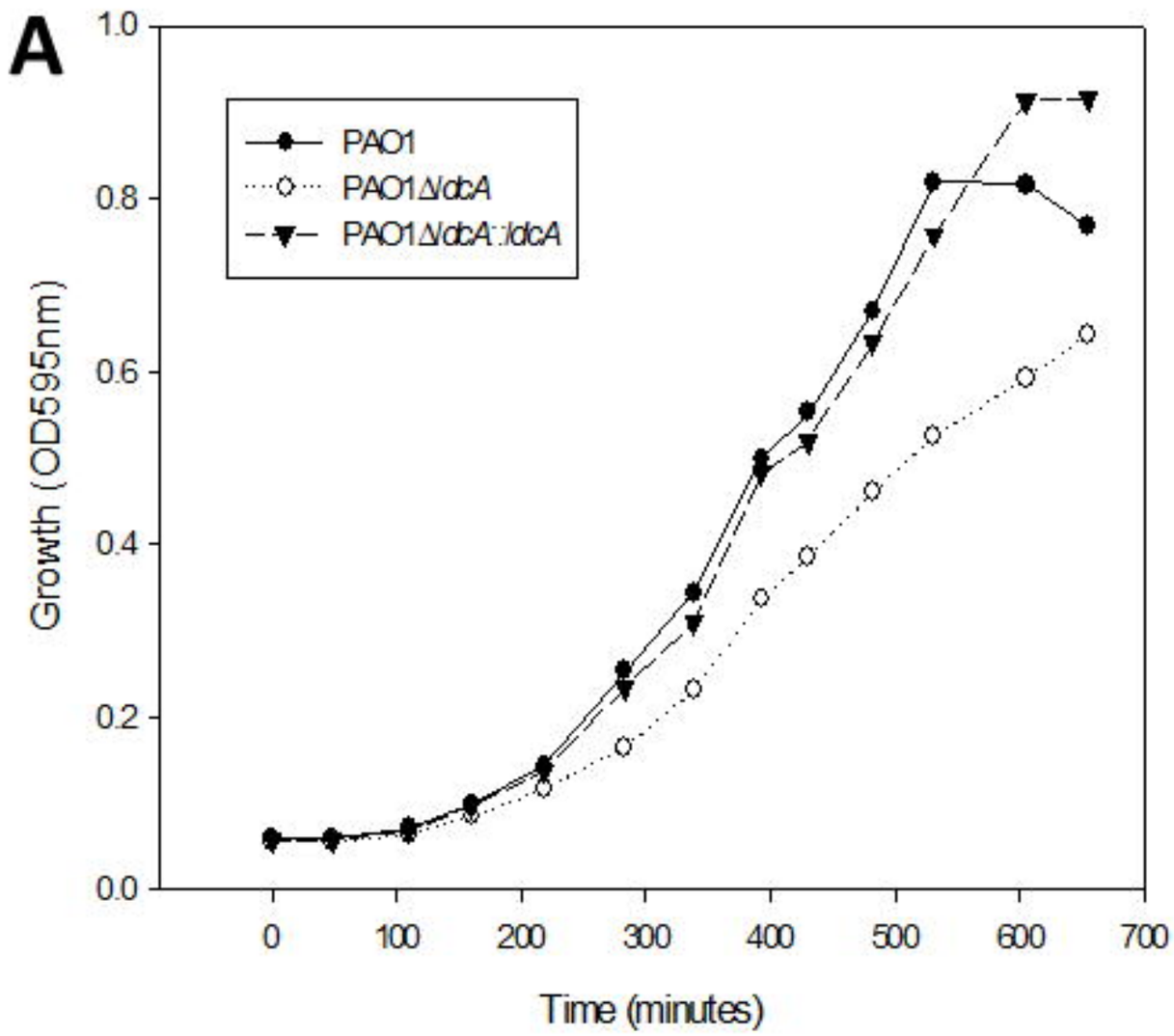
A
PAO1
PAO1Δ*dcA*
PAO1Δ*dcA*::*dcA*
Growth (OD595nm)
Time (minutes)
0.0
0.2
0.4
0.6
0.8
1.0
0
100
200
300
400
500
600
700

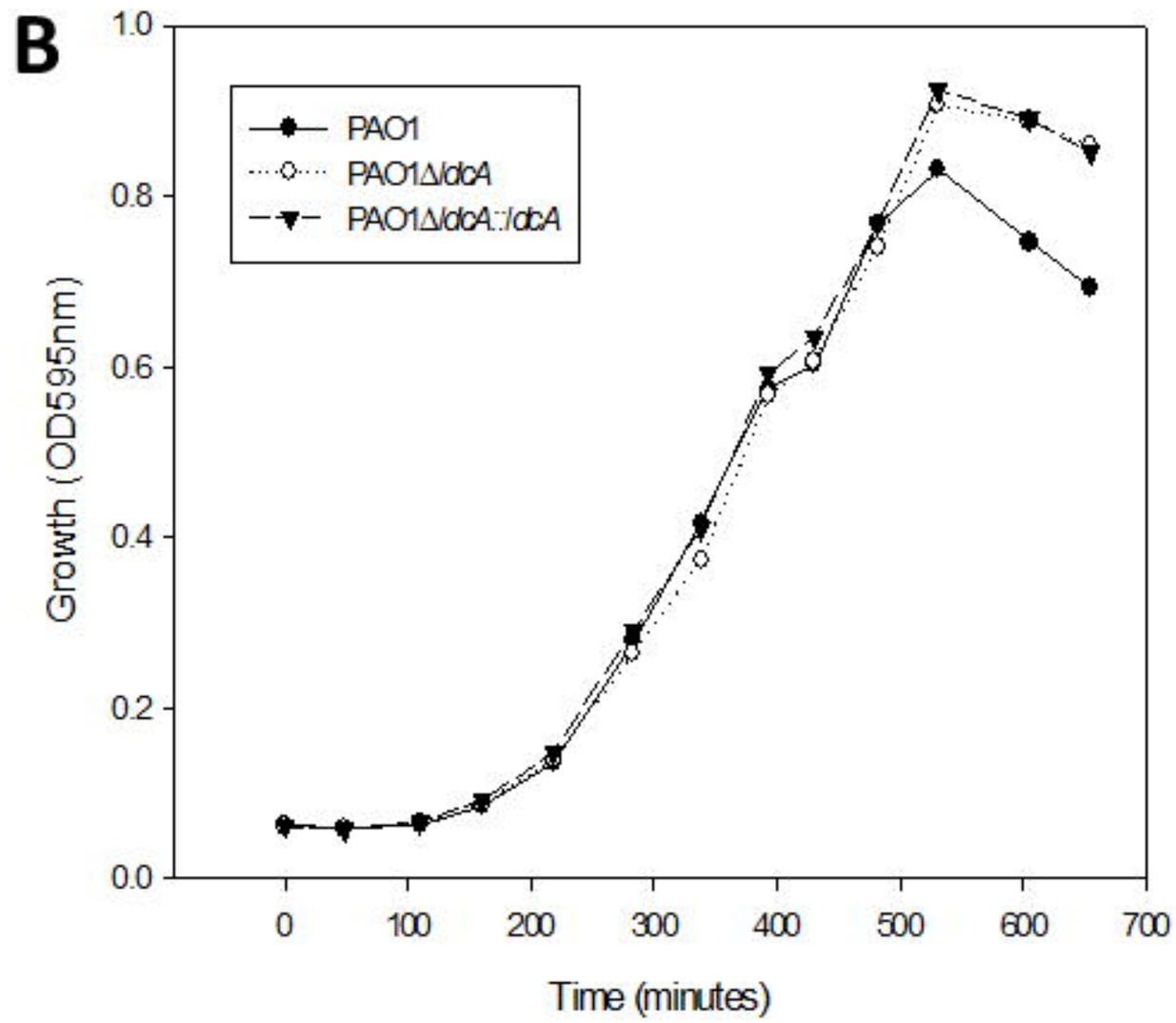
B
PAO1
PAO1Δ*dcA*
PAO1Δ*dcA*::*dcA*
Growth (OD595nm)
Time (minutes)
0.0
0.2
0.4
0.6
0.8
1.0
0
100
200
300
400
500
600
700

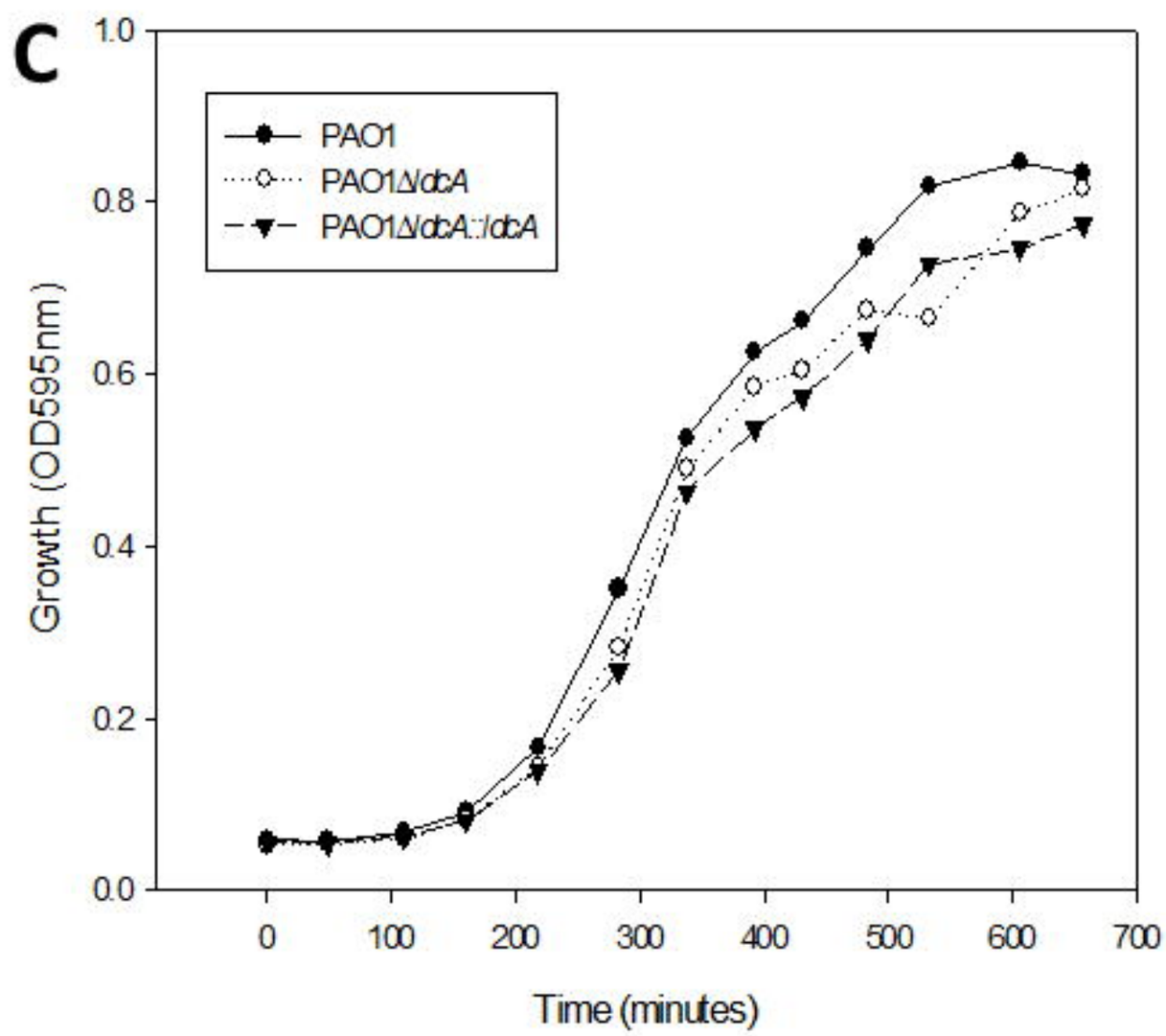
C
PAO1
PAO1Δ*dcA*
PAO1Δ*dcA*::*dcA*
Growth (OD595nm)
Time (minutes)
0.0
0.2
0.4
0.6
0.8
1.0
0
100
200
300
400
500
600
700

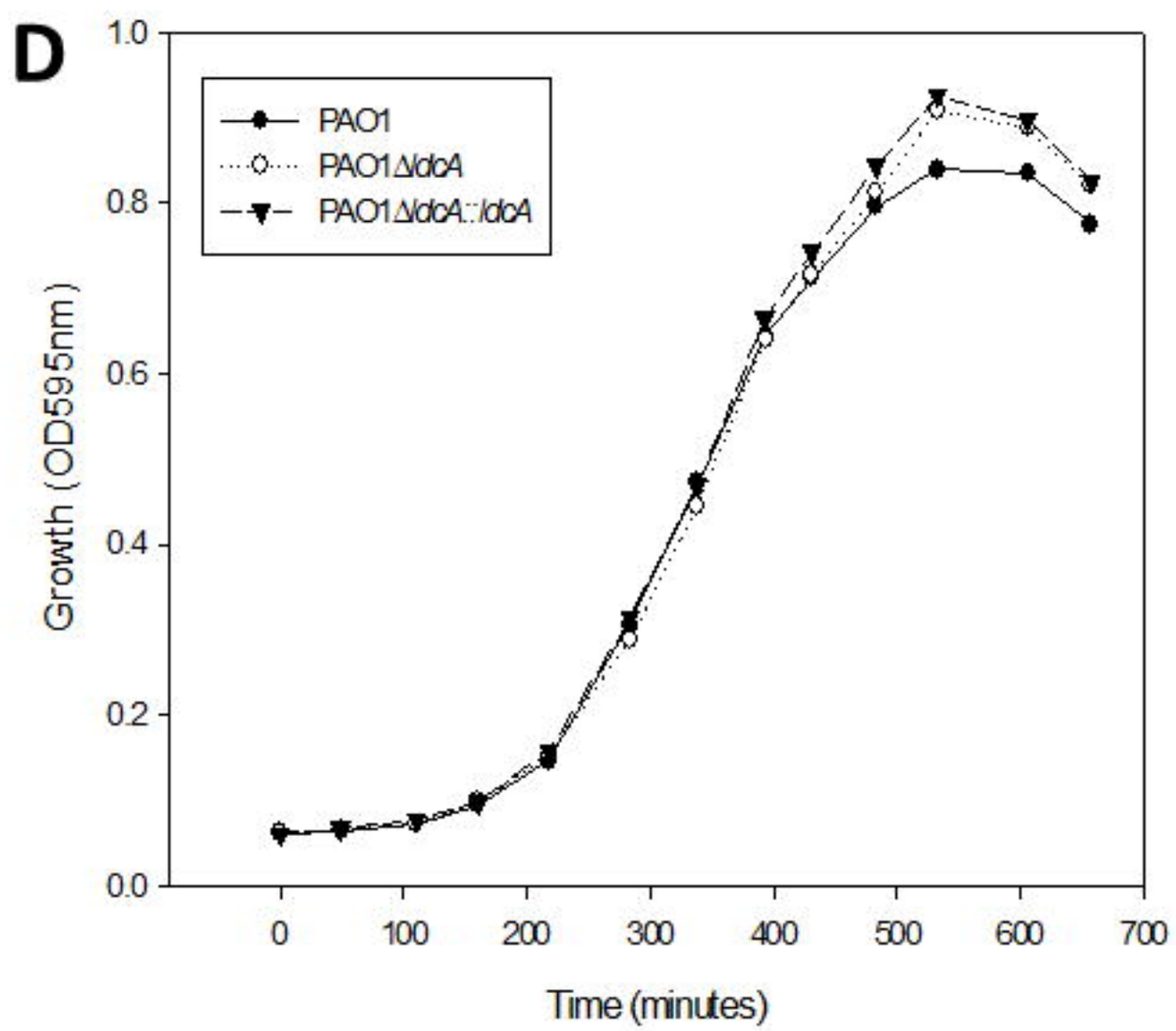
D
PAO1
PAO1Δ*dcA*
PAO1Δ*dcA*::*dcA*
Growth (OD595nm)
Time (minutes)
0.0
0.2
0.4
0.6
0.8
1.0
0
100
200
300
400
500
600
700